Journal of Medicinal Chemistry

Article

pubs.acs.org/jmc

Fragment-Based Discovery of Indole Inhibitors of Matrix Metalloproteinase-13

Steven J. Taylor,*[,†] Asitha Abeywardane,[†] Shuang Liang,[†] Ingo Muegge,[†] Anil K. Padyana,[†] Zhaoming Xiong,[†] Melissa Hill-Drzewi,[†] Bennett Farmer,[†] Xiang Li,[†] Brandon Collins,[†] John Xiang Li,[†] Alexander Heim-Riether,[†] John Proudfoot,[†] Qiang Zhang,[†] Daniel Goldberg,[‡] Ljiljana Zuvela-Jelaska,[†] Hani Zaher,[§] Jun Li,[†] and Neil A. Farrow[†]

[†]Boehringer Ingelheim Pharmaceuticals Inc., 900 Ridgebury Road, Ridgefield, Connecticut 06877-0368, United States

[‡]Karos Pharmaceuticals, 5 Science Park # 2, New Haven, Connecticut 06511, United States

[§]Eugene Applebaum College of Pharmacy and Health Sciences, 259 Mack Avenue, Detroit, Michigan 48201, United States

Supporting Information

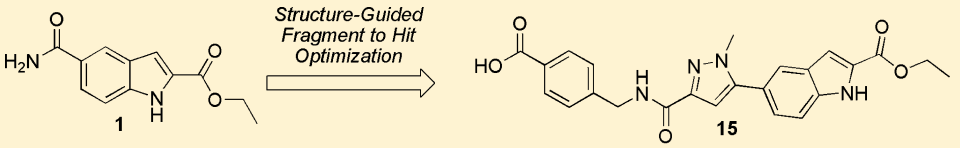

MMP-13 IC_{50} = 39 μM
MMP-2 IC_{50} = 60 μM
MMP-14 IC_{50} = >500 μM

MMP-13 IC_{50} = 0.001 μM
MMP-2 IC_{50} = 18 μM
MMP-14 IC_{50} = 8.3 μM

ABSTRACT: Matrix metalloproteases (MMPs) play an important role in cartilage homeostasis under both normal and inflamed disease states and, thus, have become attractive targets for the treatment of arthritic diseases. Herein, we describe the identification of a potent, selective MMP-13 inhibitor, developed using fragment-based structure-guided lead identification and optimization techniques. Virtual screening methods identified a novel, indole-based MMP-13 inhibitor that bound into the S1′ pocket of the protein exhibiting a novel interaction pattern hitherto not observed in MMP-13 inhibitors. X-ray crystallographic structures were used to guide the elaboration of the fragment, ultimately leading to a potent inhibitor that was >100-fold selective over nine other MMP isoforms tested.

INTRODUCTION

Fragment-Based Screening (FBS). As productivity in the pharmaceutical industry has decreased over the past 20 years, many companies have begun to seek out alternative methods for discovering druglike leads for "nondruggable" proteins to complement the traditional high-throughput screening (HTS) screening of corporate libraries. One method that has gained acceptance over the past decade is screening low molecular weight, highly soluble "fragments" against a particular target of interest.[1] These fragments are then evolved, with the aid of crystallographic costructure data, into lead chemical series. In its most simple form, fragment screening relies on triaging and prosecuting hits based more on their ligand efficiency (defined by binding free energy or potency/number of nonhydrogen atoms) rather than on their intrinsic potency.[2] A primary rationale for screening fragments [molecular weight (MW) ≤ 350 atomic mass units (AMUs)], as opposed to larger molecules, is that they access a broad chemical space (relative to molecular size), while screening a limited number of compounds. Additionally, smaller-sized fragment libraries can be prescreened for favorable physiochemical properties such as solubility, log *P*, and lack of aggregation, such that hits from a fragment screen would inherently have druglike properties embedded within the starting scaffold.[3] Fragment screens typically have a higher hit rate than traditional HTS due to the fact that smaller compounds are less likely to have mismatched, unfavorable interactions with the target protein binding site.

Fragments typically bind to their target protein with low affinity (μM to mM range); thus, a number of sensitive biophysical techniques can be leveraged to help verify and triage fragment hits prior to X-ray structure determination. Biophysical methods such as nuclear magnetic resonance (NMR),[4] surface plasmon resonance (SPR),[5] and calorimetry[6] have all been developed to detect weak interactions between fragments and their target protein. As of 2010, at least 13 compounds have been advanced into phase 1 and phase 2 clinical trials discovered with the help of fragment-based lead identification methodologies.[7]

Our strategy involved fragment virtual screening and FBS as a supplement to HTS to discover selective inhibitors of matrix metalloprotease (MMP)-13 since our HTS screening did not deliver ideal lead options. MMP-13 was viewed as an attractive target for FBS because the protein could be readily crystallized.

Inhibition of MMP-13. MMPs are zinc- and calcium-dependent peptidases, involved in the cleavage of collagen,

Received: August 23, 2011
Published: October 21, 2011

dx.doi.org/10.1021/jm201129m | J. Med. Chem. 2011, 54, 8174–8187

gelatin, and other proteins in the extracellular matrix. MMPs have been implicated in a wide range of disorders ranging from oncology to infectious diseases, and as such, a number of pan-MMP inhibitors have entered clinical trials.[8] There are approximately 23 known human MMPs that are grouped into subtypes based upon their substrates. To date, however, broad spectrum MMP inhibitors have been compromised by side effects, primarily muscular skeletal syndrome (MSS), which is characterized by painful stiffening of the joints. MSS is thought to occur by inhibition of intrinsic cellular matrix degradation, likely due to inhibition of MMPs other than MMP-13.[9] MMP-13 is the most efficient enzyme of this class at degrading collagen and has been implicated in the development of osteoarthritis and rheumatoid arthritis.[10] As such, selective inhibition of MMP-13 has become an attractive target for small molecule intervention.

While the subunits of each class of MMPs differ, the catalytic domains share the canonical zinc-binding amino acid sequence HExxHxxGxxH.[11] Classical, broad spectrum inhibitors gained potency via direct interaction with the zinc residue, which inevitably made designing selectivity into these inhibitors challenging.[12] Outside the active site, MMPs differ specifically in the S1′ pocket in a profound manner,[13] providing an opportunity to gain selectivity. MMP-13, in particular, possesses a large S1′ pocket that, when appropriately occupied by a ligand, opens up a side pocket (S1′*) not observed in many other MMPs.[14] The structural significance of this pocket has been exploited by a number of companies, resulting in potent selective MMP-13 inhibitors that do not interact with the catalytic zinc. These inhibitors share common binding motifs: An aromatic group π-stacks against histidine 222, direct or water-mediated hydrogen bonds are made with residues (threonine 245, threonine 247, and methionine 253) in the selectivity loop, and an aromatic group is located in the hydrophobic portion of the S1′* pocket formed by residues phenylalanine 217 and leucine 218.

As few examples of selective inhibitors[15] were known at the time of our internal uHTS campaign, we initiated a virtual screening and fragment-based approach to discover high ligand efficiency leads with the aim of then evolving them into selective inhibitors using structure-guided methods to complement our chemistry strategy.

RESULTS AND DISCUSSION

Prior to high concentration screening, we preformed a virtual screen of our entire corporate library to enrich our fragment screening deck with compounds that had the potential to bind within the S1′ pocket of MMP-13.[16] Our fragment library of approximately 1000 diverse scaffolds enriched with the hits from the virtual screen was screened in a MMP-13 molecular assay at high inhibitor concentration (500 μM). Among the hits were two related compounds derived from the virtual screening efforts that exhibited modest MMP-13 inhibition yet ligand efficiencies as good as those of the most potent MMP-13 inhibitors reported in the literature (**1** and **1a**). In parallel, the fragment library was screened in two additional primary assays [saturation transfer difference (STD) NMR and size exclusion chromatography mass spectrometry (SEC-MS)] to detect weak binding interactions. Fragment hits were prioritized based upon overlapping activity in the three assays as well as novelty, as defined by similarity to known MMP-13 scaffold classes. Fragments were then prosecuted in high-throughput crystallization experiments to elucidate their binding mode within the protein. While several interesting hits were identified, none were more attractive than the 5-carbamoyl-1*H*-indole-2-carboxylic acid ethyl ester identified by virtual screening (**1**, Figure 1) due to its high ligand efficiency (>0.3) in the high

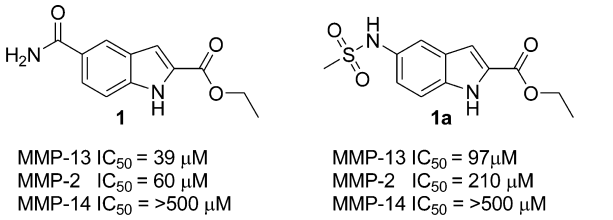

Figure 1. Indole-based fragment hits found from virtual screening with micromolar MMP activity.

concentration MMP-13 catalytic assay and novel binding mode within the S1′ pocket of MMP-13.

Figure 2a shows the binding mode of **1** as determined by X-ray crystallography. Although serendipity has played a role in virtual screening successes in the past,[17] it was still a surprise that fragment **1** was found to bind shallower in the S1′ pocket than expected. The ethyl-ester moiety binds adjacent to histidine 222, one of the three histidine residues that chelate the catalytic zinc. The indole core is positioned deeper in the S1′ pocket, with the indole nitrogen forming a hydrogen bond with the backbone carbonyl of phenylalanine 241. This interaction had not been described before in the literature of MMP-13 inhibitors. The nitrogen of the amide group engages the selectivity loop of the protein though hydrogen bonds with threonine 245 and water-mediated with threonine 247. Fragment **1** showed some modest activity over MMP-2 and -14, which was consistent with a partial occupancy of the S1′ selectivity pocket of MMP-13.

It has previously been shown that MMP-13 selectivity may be achieved when ligands bind further into the S1′ pocket, occupying the S1′* subpocket (PDB: 1XUD). Figure 2b shows an overlay of compound **1** and a selective literature inhibitor. It is apparent from the figure that the indole fragment is not accessing the region of the protein that has been reported to confer selectivity and thus providing a roadmap for increasing potency against MMP-13, while sparing activity against the other maxtix metalloproteases.

The initial structure−activity relationship (SAR) focused on determining if the ethyl ester at the 2-position of the indole was required for activity since this moiety was viewed as a potential metabolic liability. On the basis of the cocrystal structure, this functional group participates only in weak, water-mediated interactions and potential van der Waals interactions with the lipophilic side chains of the protein. The SAR in this region is shown in Table 1. Replacement of the ether oxygen with a neutral atom (−CH_2− **2**) or a hydrogen bond donor (NH, **3**) resulted in a complete loss of activity (ketone, amine, and ester are all in the planar confirmation). This finding suggested the necessity of a hydrogen bond acceptor (HBA), despite the fact that the crystal structure did not indicate any direct hydrogen bonding to the ether oxygen. Maintaining the HBA but constraining the element within a ring resulted in an analogue that retained some activity against MMP-13 (Table 1, **5**). Oxazolines similar to that in compound **5** are know to be hydrolytically liable, so further elaboration of the molecule off the 6-position of the indole was performed with the ethoxy ester as an anchoring functional group.

dx.doi.org/10.1021/jm201129m | J. Med. Chem. 2011, 54, 8174–8187

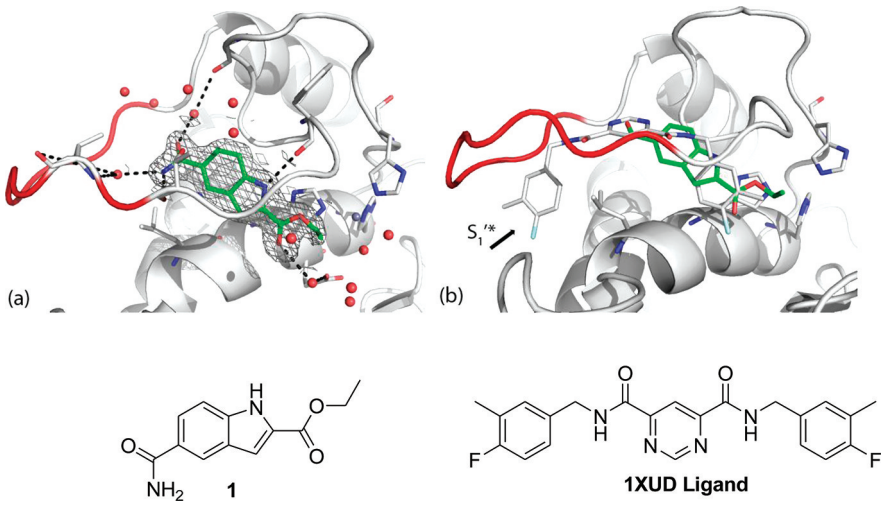

Figure 2. (a) X-ray crystal structure of **1**. The region of the protein referred to as the "selectivity loop" is colored red. The catalytic zinc atom is depicted as a gray sphere, while stably bound water molecules are shown as red spheres. (b) Overlay of **1** with the MMP-13 selective, nonzinc-chelating Aventis inhibitor (PDB: 1XUD) that accesses the S1′* pocket.

Table 1. SAR for Substitution at the 2-Position of Indole Fragment 1

Entry	Cpd.	Structure	MMP-13 IC_{50} (LE)[a]	MMP-2/14 IC_{50}
1	**1**	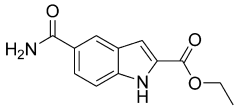	39 (0.35)	60/>500
2	**2**	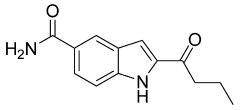	>500	>500/>500
3	**3**	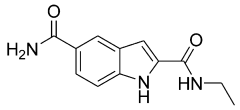	>500	>500/>500
4	**4**	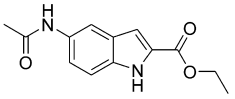	31 (0.34)	>500/>500
5	**5**	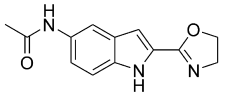	220 (0.27)	>500/>500

[a] IC_{50} values are represented as μM and averaged from a minimum of two determinations; LE calculated by $RT\ \ln(IC_{50})$/no. of heavy atoms.

On the basis of the X-ray costructure of **2** with MMP-13 and literature compounds (PDB: 1XUD), we sought to grow the fragment in the direction of the S1′* pocket to gain potency and selectivity over all other MMP isoforms. In addition to testing activity against MMP-13, compounds were tested for their ability to inhibit MMP-2 and MMP-14, two isoforms that predict selectivity against a wider panel of metalloproteases.[18] Initial attempts at increasing potency and selectivity were focused on replacing the 6-carboxamide with an aromatic ring mimicking known selective literature inhibitors.

Replacement of the carboxamide with an aryl ring was envisioned to provide a more rigid scaffold that could be further elaborated to access deep within the S1′* pocket to gain selectivity. Carboxyamide replacements are shown in Table 2.

Table 2. SAR for Substitution at the 5-Position of Indole Fragment 2

Entry	Cpd.	Structure	MMP-13 IC_{50} (LE)[a]	MMP-2/14 IC_{50}
1	**1**	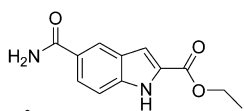	39 (0.35)	60/>500
2	**6**	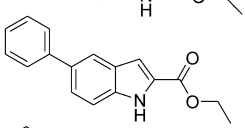	>500	>500/>500
3	**7**	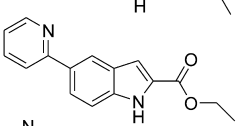	>500	>500/>500
4	**8**	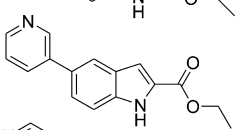	15 (0.32)	30/51
5	**9**	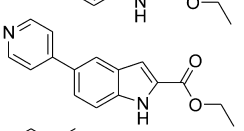	82 (0.29)	310/225
6	**10**	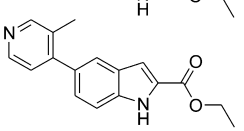	9.6 (0.32)	>500/>500
7	**11**	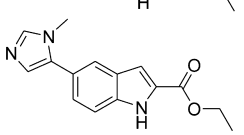	2.5 (0.38)	24/15

[a] IC_{50} values are represented as μM and averaged from a minimum of two determinations; LE calculated by $RT\ \ln(IC_{50})$/no. of heavy atoms.

Simple replacement of the amide with a phenyl analogue resulted in complete loss of enzyme inhibition. Adding a heteroatom to the ring resulted in increased potency with the 3- and 4-pyridyl analogues (Table 2, entries 4 and 5), presumably due to a hydrogen bond interaction with the side chain of threonine 247, which is not available when the HBA is α to the attachment indole ring (Table 2, entry 3). Substitution on the distal aryl ring α to the biraryl connection was envisioned to

dx.doi.org/10.1021/jm201129m | J. Med. Chem. 2011, 54, 8174–8187

increase potency by (A) twisting the aromatic ring out of plane to give a dihedral angle of 46°, the more preferred 40° mirroring the angle observed in the advanced literature inhibitors, and (B) positioning a small lipophilic group in the direction of a small lipophilic notch generated by proline 255 not seen in other MMPs. Methyl pyridyl **10** and *N*-methyl imidazole **11** were both tolerated and showed increased molecular potency. In addition, selectivity against MMP-2 and -14 was >10-fold. To confirm this increase in potency and selectivity, a crystal structure of imidazole **11** was obtained (Figure 3). The crystal structure revealed that the gain in selectivity is likely due to the positioning of the methyl group in an MMP-13-specific pocket formed by the presence of proline 255.

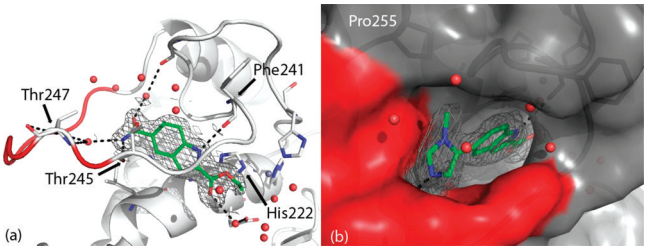

Figure 3. (a) Costructure of **11** bound to MMP-13 and (b) the imidazole methyl group is directed into a subpocket of S1′, toward residue Pro255.

Guided by the costructure of compound **11**, we further elaborated the core scaffold to determine if additional potency and selectivity could be obtained by fully occupying the S1′* pocket of the enzyme (Table 3). To access the S1′* pocket necessitated substitution of the 3-position of the imidazole; thus, we exchanged the imidazole core for a pyrazole. This modification had the additional benefit of allowing for another interaction between the pyrazole nitrogen and a tightly bound water within the active site. Substitution off of the aryl ring with a carboxyl group was tolerated (**12**), which, based on modeling, provided a synthetic handle for further elaboration into the S1′* subpocket. In addition, this modification maintained some selectivity against MMP-2 and -14. Following SAR from previous inhibitors, the ester was replaced with a benzyl amide containing various distal HBAs at the 4-postion of the aromatic ring. The amide modification was hypothesized to rigidify the core structure, reinforcing the water-mediated hydrogen bond to the pyrazole and define the proper trajectory of the aryl ring and placement of the HBA in proximity to interact with Lys140. The simple 4-pyridyl amide (Table 3, **13**, entry 2) provided the first submicromolar MMP-13 inhibitor and displayed strong selectivity over MMP-2 and -14 (>5000-fold). A similar increase in potency was observed with the pyridine core (compound **17**), which had comparable potency to the pyrazole core but with slightly lower ligand efficiency. Excising the HBA out of the ring by replacing the pyridine ring with a pyridone moiety (**14**) resulted in an analogue that maintained potency and some selectivity over MMP-12 and -14 (Table 3, entry 3). Replacement of the hydrogen bond donor (HBD) with a carboxylic acid further improved the potency of the inhibitors approximately 10-fold, presumably by interacting via a salt bridge with Lys140 (Table 3, **15**, entry 4). Extending the carboxylate moiety one methylene carbon away from the aromatic ring (**16**) resulted in a slight decrease in potency, highlighting the importance of placement of the carboxylate relative to the rest of the scaffold. All of the compounds showed selectivity over MMP-2 and -14, validating the strategy of occupying the S1′* pocket as a means to achieve selectivity with little shift in the presence of exogenous protein highlighting their potential.

To confirm the binding interactions leveraged by the elaborated molecules in Table 3 and to further optimize these analogues, a costructure of compound **15** was obtained (Figure 4). The structure revealed that the terminal benzoic acid of the compound accesses the S1′* pocket. The terminal acid moiety makes a direct hydrogen bond with the Nz nitrogen of lysine 140, and water mediated interactions with the backbone carbonyl of serine 209 and the hydroxyl group of tyrosine 246. Additionally, the inhibitor's position in the S1′ pocket is reinforced by two water-mediated hydrogen bond interactions with the backbone amide nitrogen of Met253 and a direct hydrogen bond interaction with the backbone amide nitrogen of threonine 274.

On the basis of its excellent potency and selectivity profile, compound **15** was further profiled in more physiologically relevant metalloprotease assays as well as advanced into pharmacokinetic profiling. Compound **15** was potent in a full-length MMP-13 collagen degradation assay (11 nM) and was able to inhibit degradation of bovine nasal cartilage with an IC_{50} of 31 nM. In addition **15** was >1000× selective over nine other MMPs tested (Figure 5). Passive permeability was predicated to be high, based upon parallel artificial membrane permeability assay (PAMPA) data (data not show); however, significant efflux was observed in human CACO-2 cells, which is consistent with compounds with comparable polar surface areas (PSAs) to **15**. The in vitro profile was acceptable in h/rLM, even with the perceived ester as a liability, and as such, this analogue was moved into rat pharmacokinetics. When dosed orally at 10 mpk (iv 1 mpk), compound **15** reached micromolar plasma levels, displayed modest clearance, and showed acceptable bioavailability (39%). The V_{ss} of the compound was quite low at 0.26, in line with other carboxylic containing compounds. To better understand the metabolic fate of **1**, a metabolic ID study upon incubation with rat liver microsomes was performed. The major metabolite was the result of ester hydrolysis to give **18** (Table 4, entry 2), which accounted for >80% of all metabolites formed.

A number of analogues were generated to follow up on the observed primary metabolite of **15** (Table 4). The diacid metabolite (**18**) was inactive against MMP-13, reiterating the importance of this ester functional group. Strikingly, complete removal of this functional group, representing removal of only four atoms in the molecules, resulted in a complete loss of MMP-13 inhibition. Replacement of the ester, with an ethyl ether that contained the acceptor but not the carboxyl group, partially recovers some the activity lost upon remove of the ester (Table 4, **20**, entry 4). These experiments highlight the critical contribution of this moiety to overall activity, despite the limited direct interactions observed between the ester and the protein.

Chemistry. Compounds **1**[19] and **5**[20] were synthesized as described previously, and compound **4** was purchased directly from commercial vendors. The synthesis of compound **2** is illustrated in Scheme 1. Weinreb's amide formation from acid **21** generated amide **22**, which was treated with propylmagnesiumbromide, giving the intermediate ketone **23**. Palladium-catalyzed aminocarbonalytion reaction from the corresponding keto bromide **23** provided compound **2**.

dx.doi.org/10.1021/jm201129m|*J. Med. Chem.* 2011, 54, 8174–8187

Table 3. SAR of Fully Elaborated Analogs of Indole Fragment 1

Entry	Cpd.	Structure	MMP-13 IC_{50} (LE)[a]	MMP-13(S) IC_{50}[b]	MMP-2/14 IC_{50}
1	**12**	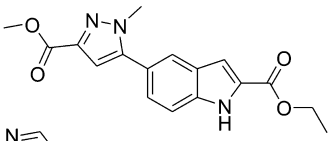	2.4 (0.32)	NT	83/41
2	**13**	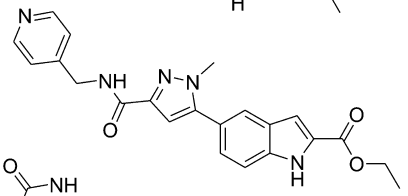	0.09 (0.32)	0.36	>500/>500
3	**14**	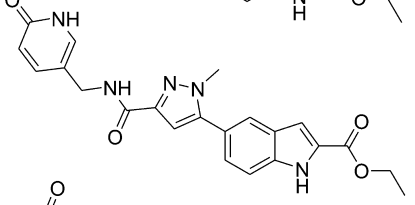	0.12 (0.30)	0.28	>24/11
4	**15**	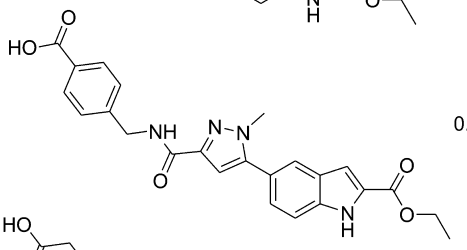	0.001(0.37)	0.004	18/8.3
4	**16**	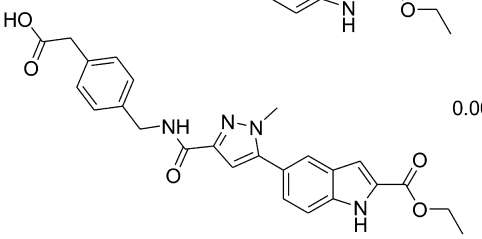	0.003 (0.34)	0.014	>22/>22
5	**17**	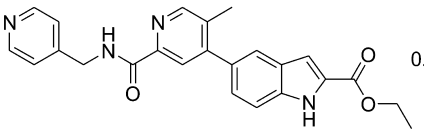	0.15 (0.3)	0.64	>20/>22

[a] IC_{50} values are represented as μM and averaged from a minimum of two determinations; LE calculated by $RT \ln(IC_{50})$/no. of heavy atoms. [b] IC_{50} in MMP-13 molecular assay with the addition of 1.25% purified human serum albumin.

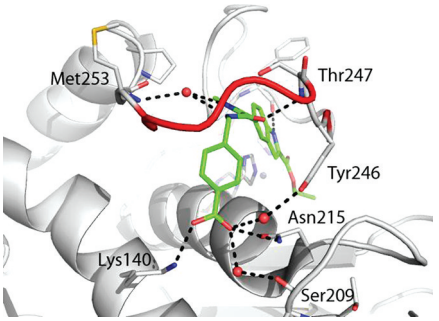

Figure 4. Costructure of compound **15** showing the network of hydrogen bond interactions formed between the inhibitor and the residues in the S1′* pocket of the protein.

The synthesis of compound **3** is illustrated in Scheme 2. Bromide **21** was converted to the amide **24** and then treated under aminocarbonylation conditions generating compound **3**.

The synthesis of compounds **6**−**11** is illustrated in Scheme 3. 5-Aryl indole **6** was synthesized from 5-bromo-1*H*-indole-2-carboxylic acid ethylester and the corresponding aryl boronic acid via a palladium-mediated cross-coupling reaction. Alternatively, compounds **7**−**11** were generated by converting 5-bromo-1*H*-indole-2-carboxylic acid ethyl ester (**25**) to the corresponding boronic ester **26** and then coupling directly with various aryl bromides.

The synthesis of compound **12** is illustrated in Scheme 4. Methylhydrazine was condensed with the but-2-ynedioic acid dimethyl ester, and the intermediate was heated to evolve water generating hydroxypyrazole **27**. This alcohol was converted to the pyrazole bromide **28**, which was then coupled with intermediate **26** to give the corresponding indole **12**.

The synthesis of compounds **13**−**16** is illustrated in Scheme 5. Ester **28** was hydrolyzed to the corresponding acid, which was then coupled with various amines to give substituted benzylamides. The esters **32** and **34** were hydrolyzed under basic conditions. The aryl bromides were coupled with **26** to generating the corresponding elaborated indole analogues.

The synthesis of compound **17** is shown in Scheme 6. Under palladium-catalyzed conditions, chloropyridine **36** was coupled with indole boronic ester **6** and then treated with 2-(1*H*-7-azabenzotriazol-1-yl)-1,1,3,3-tetramethyl uronium hexafluoro-

dx.doi.org/10.1021/jm201129m | *J. Med. Chem.* 2011, 54, 8174−8187

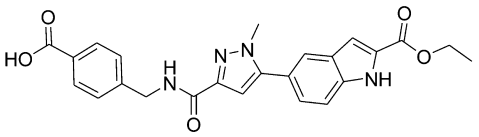

MMP IC_{50} (μM)	1	2	3	7	8	9	10	12	13	14	13(+HSA)
	>22	18	>22	>22	>22	8.9	16	>22	0.001	8.3	0.004

target independent in vitro profile	
Cyp 2C9 IC_{50} (μM) =	> 30
Cyp 3A4 IC_{50} (μM) =	> 30
h/r LM (%Q_H) =	40/41
aq sol 7.4 (μg/mL) =	60
CACO-2 (AB/ ER) =	0.6/ 26
logP =	1.9
PSA =	126
MW =	446

MMP-13 IC_{50} Full length (μM) =	0.011
BNC degradation IC_{50} (μM) =	0.031

rat in vivo pharmacokenetic profile	
iv AUC (nM h/mL)	1109 +/- 64
VSS (mL/mi/kg)	0.26
CL (mL/min/kg)	34
T1/2 (h)	0.47
Cmax (nM)	1,657
po AUC (nM h/mL)	4,328
%F	39

Figure 5. Extended profiling of **15** and rat pharmacokinetic profile.

Table 4. Ester SAR on Elaborated Molecules

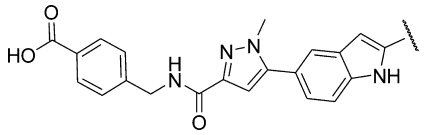

Entry	Cpd.	R	MMP-13 IC_{50}(LE)[a]	MMP-13 IC_{50}(HSA)[b]	hLM (%Q_H)[c]
1	**15**		0.001 (0.37)	0.004	40
2	**18**		25 (0.22)	56	NT
3	**19**		>26	NT	25
4	**20**		0.25 (0.28)	1.9	78

[a] IC_{50} values are represented as μM and averaged from a minimum of two determinations; LE calculated by $RT \ln(IC_{50})$/ no. of heavy atoms. [b] IC_{50} in MMP-13 molecular assay with the addition of 1.25% purified human serum albumin. [c] In vitro assessment of metabolic stability of compounds in the presence of isolated human liver microsome preparations. Data are reported as a % relative to human hepatic blood flow.

phosphate methanaminium (HATU) and the methyleneaminopyridine to generate **17**.

The synthesis of compound **18** is illustrated in Scheme 7. Compound **15** was saponified to **18** under aqueous basic conditions.

The synthesis used to generate pyridine analogue **19** is shown in Scheme 8. Intermediate bromide **33** was coupled with the 5-indole boronic acid under typical conditions to provide the elaborated molecule **19**.

The synthesis used to generate ether analogue **20** is illustrated in Scheme 9. Commercially available indole **25** was protected with an ethylene trimethylsiloxymethyl (SEM) group, and the ester was reduced to the primary alcohol **39**. The alcohol was alkylated (**40**), and the bromide was converted to the boronic acid (**41**). The boronic acid was coupled with intermediate **33**, and the SEM group was removed under fluoride conditions to provide compound **20**.

CONCLUSIONS

As compared with the starting indole fragment **1**, compound **15** represents a 39000-fold increase in potency while maintaining the original high ligand efficiency (>0.3). Using costructures of intermediates and known literature SAR, the indole fragment was rapidly optimized to a picomolar inhibitor that displayed a promising pharmacokinetic profile. The described study demonstrates how a novel chemical series can be obtained via combined virtual screening and fragment-based drug discovery strategies guided by high-resolution crystal structures and subsequent optimization. Fragment **1** was submitted as a synthetic intermediate for a BIPI legacy program and qualified for our fragment library due to its intrinsic solubility and low MW. The study herein highlights how every compound and intermediate that a chemist generates should be submitted for testing, regardless of pedigree or perceived limited value due to molecular size.

EXPERIMENTAL SECTION

Chemistry General Remarks. Starting materials were obtained from commercial suppliers and used without further purification unless otherwise stated. ^{1}H NMR spectra were recorded on a Bruker UltraShield 400 MHz spectrometer operating at 400 MHz in solvents, as noted. Proton coupling constants (J values) are rounded to the nearest Hz. All coupling constants are reported in hertz (Hz), and multiplicities are labeled s (singlet), bs, (broad singlet), d (doublet), t (triplet), q (quartet), dd (doublet of doublets), dt (doublet oftriplets), and m (multiplet). All NMR spectra were referenced to

dx.doi.org/10.1021/jm201129m | J. Med. Chem. 2011, 54, 8174–8187

Scheme 1. [a]

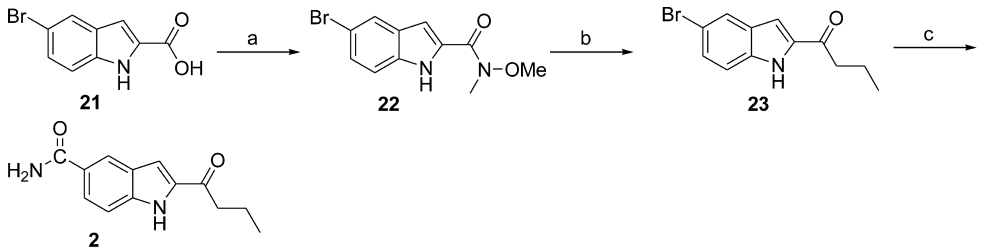

[a]Reagents and conditions: (a) TBTU, *N,N*-methoxy methylamine, DIEA, DMF. (b) nPrMgCl, THF/DMF. (c) $Mo(CO)_6$, DBU, Herrmann's Palladacycle, DIEA, HCl dioxane water.

Scheme 2. [a]

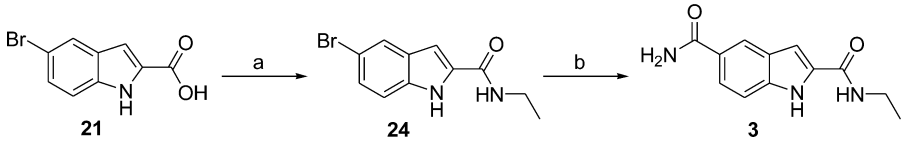

[a]Reagents and conditions: (a) TBTU, ethylamine, THF/DMF. (b) $Mo(CO)_6$, DBU, Hermann's Palladcycle, DIEA, HCl 1,4-dioxane, water.

Scheme 3. [a]

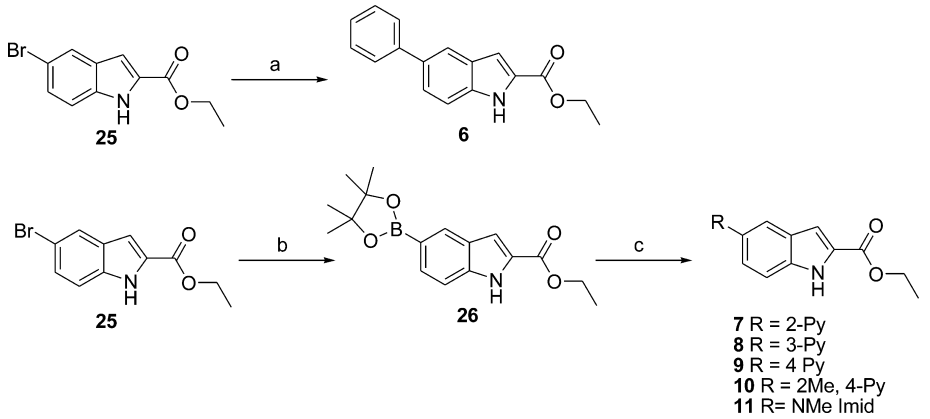

[a]Reagents and conditions: (a) $PhB(OH)_2$, bistriphenylphosphine palladium(II) chloride, DMF, 2 M aqueous Na_2CO_3. (b) Bis(dipinacolyl)borane Pd(dppf)Cl, 1,4-dioxane. (c) Ar-X, bis(triphenylphosphine)palladium(II) chloride, DMF, 2 M aqueous Na_2CO_3.

Scheme 4. [a]

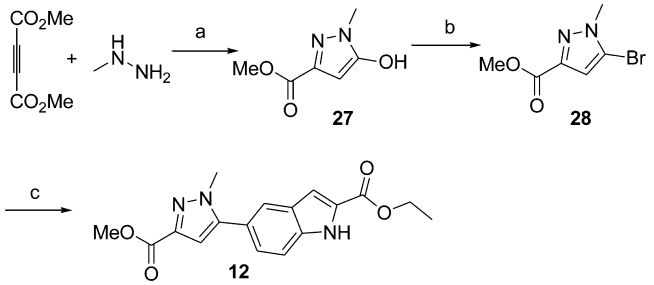

[a]Reagents and conditions: (a) Diethyl ether, 0 °C, filter, 100 °C neat. (b) $POBr_3$, 80 °C. (c) Compound **26**, $Pd(PPh_3)_2$ Cl_2, DMF, 2 M aqueous Na_2CO_3.

tetramethylsilane (TMS δH 0, δC 0). All solvents were HPLC grade or higher. The reactions were followed by TLC on precoated Uniplate silica gel plates purchased from Analtech. The developed plates were visualized using 254 nm UV illumination or by PMA stain. Flash column chromatography on silica gel was performed on Redi Sep prepacked disposable silica gel columns using an Isco Combiflash, Biotage SP1, or on traditional gravity columns. Reactions were carried out under an atmosphere of Ar at room temperature, unless otherwise noted. Mass spectroscopy data were obtained using the Micromass Platform LCZ (flow injection). In addition to mass spectrometry and NMR, purity (confirming ≥95% purity) was evaluated by the following systems.

System 1. Analytical HPLC using a Varian Dynamax SD-200 pump coupled to a Varian Dynamax UV-1 detector: The solvents were the following: (A) water + 0.05% TFA and (B) acetonitrile + 0.05% TFA; flow, 1.2 mL/min. Column Vydac RP-18, 5 m, 250 mm × 4.6 mm, photodiode array detector at 220 nm; from 95 to 20% solvent (A) over 25 min confirming ≥95% purity.

System 2. HP 1110 Agilent LCMS using a Quaternary G1311A pump coupled to a Micromass Platform LCZ detector: The solvents were as follows: (A) water + 0.1% formic acid and (B) acetonitrile + 0.1% formic acid; flow, 1.5 mL/min. Photodiode array detector at 190 or 400 nm (a) Agilent Zorbax Eclipse XDB-C8 5 μm, 4.6 mm × 150 mm column, 4.6 mm × 30 mm, 3.5 μm, from 99 to 5% solvent (A) over 10 min; or (b) Column Agilent Zorbax C18 SB 3.5 μm, 4.6 mm × 30 mm cartridge, from 95 to 5% solvent (A) over 2.5 min confirming ≥95% purity.

Chemstry. *2-Butyryl-1H-indole-5-carboxylic Acid Amide (2).* A solution of 5-bromo-1*H*-indole-2-carboxylic acid **21** (500 mg, 2.1 mmol), *N,N*-diisopropylethylamine (DIEA) (960 mL, 5.2 mmol), and *O*-(benzotriazol-1-yl)-*N,N,N′,N′*-tetramethyluronium tetrafluoroborate

dx.doi.org/10.1021/jm201129m|*J. Med. Chem.* 2011, 54, 8174–8187

Scheme 5. [a]

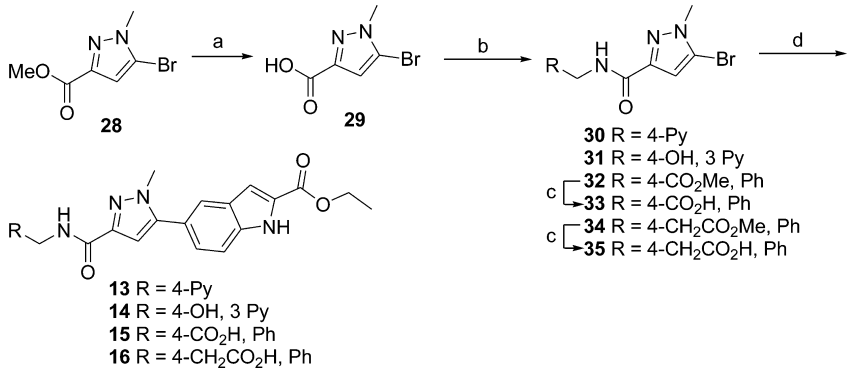

[a]Reagents and conditions: (a) LiOH, THF 1,4-dioxane, water. (b) HATU, DIEA, amine, DMF. (c) LiOH, water, THF 1,4-dioxane, methanol. (d) Compound **26**, $Pd(PPh_3)_2$, Cl_2, DMF, 2 M aqueous Na_2CO_3.

Scheme 6. [a]

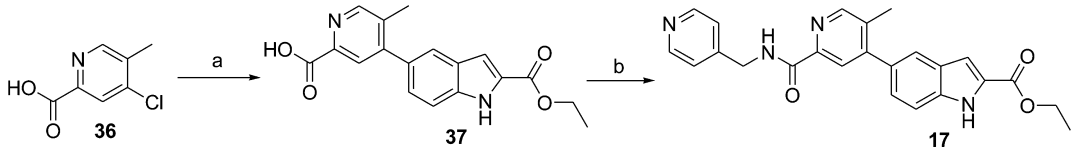

[a]Reagents and conditions: (a) Compound **26**, $Pd(4Me_2NPh, PBu)_2BF_4$, DMF, 2 M aqueous Na_2CO_3. (b) HATU, DIEA, amine, DMF.

Scheme 7. [a]

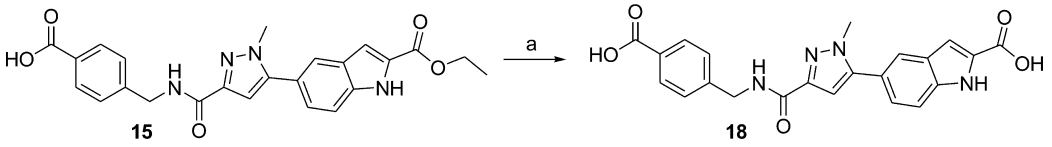

[a]Reagents and conditions: (a) LiOH, THF 1,4-dioxane, water.

Scheme 8. [a]

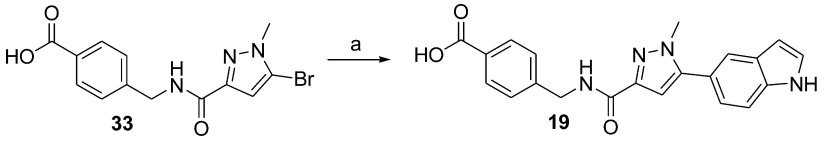

[a]Reagents and conditions: (a) $Pd(PPh)_4$, 5-indoleboronic acid, THF, 2 M aqueous Na_2CO_3.

(TBTU) (740 mg, 2.2 mmol) was charged with methoxy methylamine hydrochloride (220 mg, 2.2 mmol), and the reaction was diluted with dimethylformamide (DMF) (10 mL) and stirred for 16 h at room temperature. The reaction was quenched with water (25 mL), and the product was extracted into EtOAc. The organic layer was dried over sodium sulfate and reduced to a minimum volume by rotary evaporation. The residue was purified on silica (heptanes/EtOAc) to give 5-bromo-1*H*-indole-2-carboxylic acid methoxy-methyl-amide **22** (420 mg, 71%). ^{1}H NMR (400 MHz, DMSO-d_6): δ 11.78 (s, 1H), 7.88 (d, J = 1.6 Hz, 1H), 7.43 (d, J = 8.8 Hz, 1H), 7.33 (dd, J = 8.8 Hz, 2.0 Hz, 1H), 7.14 (d, J = 2.0 Hz, 1H), 3.80 (s, 3H), 3.34 (s, 3H).

A mixture of 5-bromo-1*H*-indole-2-carboxylic acid methoxy-methyl-amide **22** (200 mg, 0.7 mmol) was dissolved in 10 mL of tetrahydrofuran (THF) and cooled to 0 °C. Propylmagnesiumbromide (2.8 mL 5.7 mmol) was added, and the reaction was warmed to room temperature overnight. The reaction was quenched with 0.5 M HCl, and the product was extracted into EtOAc. The organic layer was dried over sodium sulfate and reduced to minimum volume by rotary evaporation. The residue was added to a 20 g prepacked silica column and eluted with EtOAc in heptanes to give 5-bromo-2-(1-methylene-butyl)-1*H*-indole **23** (103 mg, 53%). ^{1}H NMR (400 MHz, DMSO-d_6): δ 11.98 (s, 1H), 7.96 (s, 1H), 7.44−7.45 (m, 2H), 7.39 (d, J = 2.0 Hz, 1H), 3.00 (t, J = 7.2 Hz, 2H), 1.77 (m, 2H), 1.00 (t, J = 7.6 Hz, 3H).

A solution of 5-bromo-2-(1-methylene-butyl)-1*H*-indole **23** (103 mg, 0.4 mmol), molybdenum hexacarbonyl (52 mg, 0.2 mmol), and Hermann's palladcycle (37 mg, 0.04 mmol) in THF (2 mL) was added 1,8-diazabicyclo[5.4.0]undec-7-ene (DBU) (120 μL, 0.8 mmol), and the reaction vessel was sealed and heated in a microwave reactor at 150 °C for 20 min. The reactions vessel was cooled, filtered, and diluted with DMSO HCl/water and purified on reverse-phase LC to give the title compound as a white solid. (0.01 g, 10%). LCMS (ES+) m/z found, 231; retention time, 0.60 min. $C_{13}H_{14}N_2O_2$ requires 231. HPLC retention time, 7.74 min. ^{1}H NMR (400 MHz, DMSO-d_6): δ 11.92 (s, 1H), 8.29 (s, 1H), 7.93 (bs, 1H), 7.82 (dd, J = 8.8 Hz, 1.6 Hz, 1H), 7.47 (d, J = 1.6 Hz, 1H), 7.44 (d, J = 8.8 Hz, 1H), 7.20 (bs, 1H), 2.97 (t, J = 7.2 Hz, 2H), 1.70 (m, 2H), 0.96 (t, J = 7.6 Hz, 3H).

*1H-Indole-2,5-dicarboxylic Acid 5-Amide 2-Ethylamide (**3**).* A solution of 5-bromo-1*H*-indole-2-carboxylic acid **21** (500 mg, 2.1 mmol), DIEA (960 mL, 5.2 mmol), and TBTU (740 mg, 2.2 mmol) was charged with ethyl amine (1.1 mL of 1 M in THF, 2.2 mmol), and the reaction was diluted with DMF (10 mL) and stirred for 16 h at room temperature. The reaction was quenched with water (25 mL),

dx.doi.org/10.1021/jm201129m | J. Med. Chem. 2011, 54, 8174–8187

Scheme 9. [a]

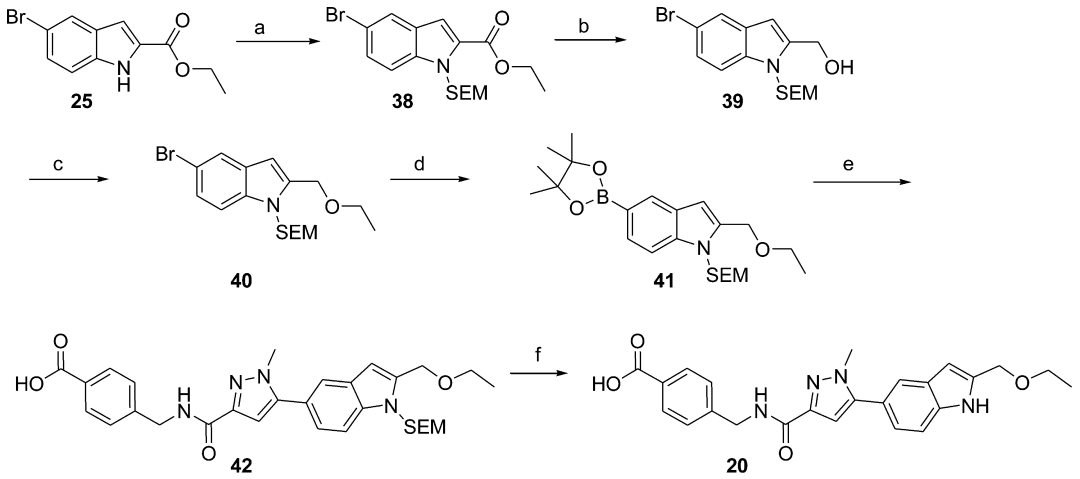

[a]Reagents and conditions: (a) SEM-Cl, THF, NAH. (b) $LiAlH_4$, THF. (c) Ag_2O, EtI. (d) Bis(dipinacolyl)borane Pd(dppf)Cl, 1,4-dioxane. (e) Compound **33**, $Pd(PPh_3)_2$ Cl_2, DMF, 2 M aqueous Na_2CO_3. (f) TBAF, ethylenediamine, THF.

and the product was extracted into EtOAc. The organic layer was dried over sodium sulfate and reduced to minimum volume by rotary evaporation. The residue was purified on silica (heptanes/EtOAc) to give 5-bromo-1*H*-indole-2-carboxylic acid ethylamide **24** as a yellow oil (500 mg, 89%). ^{1}H NMR (400 MHz, DMSO-d_6): δ 11.76 (s, 1H), 8.55 (t, J = 5.2 Hz, 1H), 7.83 (s, 1H), 7.38 (d, J = 8.8 Hz, 1H), 7.28 (dd, J = 8.8 Hz, 2.0 Hz, 1H), 7.08 (d, J = 2.4 Hz, 1H), 3.30 (q, J = 7.2 Hz, 2H), 7.14 (t, J = 7.2 Hz, 3H).

To a solution of 5-bromo-1*H*-indole-2-carboxylic acid ethylamide **24** (213 mg, 0.8 mmol), molybdenum octacarbonyl (105 mg, 0.4 mmol), and Hermann's palladcycle (37 mg, 0.04 mmol) in THF (2 mL) was added DBU (120 μL, 0.8 mmol), and the reaction vessel was sealed and heated in a microwave reactor at 150 °C for 20 min. The reaction vessel was cooled, filtered, and diluted with DMSO and HCl/water and purified on reverse-phase HPLC to give the title compound as a white solid (0.025 g, 14%). LCMS (ES+) m/z found, 232; retention time, 0.39 min. $C_{12}H_{13}N_3O_2$ requires 232. HPLC retention time, 5.44 min. ^{1}H NMR (400 MHz, DMSO-d_6): δ 11.78 (s, 1H), 8.54 (t, J= 5.6 Hz, 1H), 8.22 (s, 1H), 7.87 (brd, 1H), 7.73 (dd, J = 8.4 Hz, 1.6 Hz, 1H), 7.42 (d, J = 8.4 Hz, 1H), 7.20, (d, J = 1.6 Hz, 1H), 7.14 (brd, 1H), 3.33 (m, 2H), 1.16 (t, J = 3.6 Hz).

*5-Phenyl-1H-indole-2-carboxylic Acid Ethyl Ester (**6**).* A 5 mL microwave vial was charged with phenylboronic acid (45 mg, 0.37 mmol), 5-bromo-1*H*-indole-2-carboxylic acid ethyl ester **25** (100 mg, 0.37 mmol), and bis(triphenylphosphine)palladium(II) chloride (25 mg, 0.03 mmol). The solids were suspended in DMF (2 mL), and 2 M sodium carbonate solution (2 mL) was added to the reaction vessel. The vial was sealed and heated in a microwave reactor at 100 °C for 20 min. The reaction vessel was cooled and filtered though Celite, and the Celite was washed well with EtOAc. The combined extracts were washed with water, dried (Na_2SO_4), filtered, and evaporated in vacuo to give the crude product that was purified on reverse-phase HPLC to give the title compound **6** as a white solid (0.026 g, 26%). LCMS (ES +) m/z found, 266; retention time, 1.11 min. $C_{17}H_{15}NO_2$ requires 266. HPLC retention time, 13.25 min. $C_{17}H_{15}NO_2$ requires 266. ^{1}H NMR (400 MHz, DMSO-d_6): δ 11.95 (s, 1H), 7.93 (s, 1H), 7.67 (d, J= 7.2 Hz, 2H), 7.58 (dd, J = 8.8 Hz, 1.6 Hz, 1H), 7.53 (d, J = 8.8 Hz, 1H), 7.45 (t (dd), J = 7.2 Hz, 2H), 7.32 (t, J = 7.2 Hz, 1H), 7.21 (d, J = 2.0 Hz, 1H), 4.35 (q, J = 7.2 Hz, 2H), 1.35 (t, J = 7.2 Hz, 3H).

*5-Pyridin-2-yl-1H-indole-2-carboxylic Acid Ethyl Ester (**7**).* A 5 mL microwave vial was charged with 5-(4,4,5,5-tetramethyl-[1,3,2]-dioxaborolan-2-yl)-1*H*-indole-2-carboxylic acid ethyl ester **25** (100 mg, 0.31 mmol), 2-bromopyridine (0.03 mL, 0.31 mmol), and bistriphenylphosphine palladium(II) chloride (25 mg, 0.03 mmol). The solids were suspended in DMF (2 mL), and 2 M sodium carbonate solution (2 mL) was added to the reaction vessel. The vial was sealed and heated in a microwave reactor at 100 °C for 20 min. The reaction vessel was cooled and filtered though Celite, and the Celite was washed well with EtOAc. The combined filtrates were washed with water, dried (Na_2SO_4), filtered, and evaporated in vacuo to give the crude product that was purified on reverse-phase HPLC to give the title compound **7** as a white solid (0.020 g, 24%). LCMS (ES +) m/z found, 267; retention time, 0.63 min. $C_{16}H_{14}N_2O_2$ requires 267. HPLC retention time, 7.42 min. ^{1}H NMR (400 MHz, DMSO-d_6): δ 12.14 (s, 1H), 8.71 (bs, 1H), 8.41 (s, 1H), 8.10 (bs, 2H), 8.00 (dd, J = 8.4 Hz, 1.6 Hz, 1H), 7.58 (d, J = 8.8 Hz, 1H), 7.51 (bs, 1H), 7.28 (d, J = 1.6 Hz, 1H), 4.37 (q, J = 3.2 Hz, 2H), 1.36 (t, J = 3.2 Hz, 3H).

*5-Pyridin-3-yl-1H-indole-2-carboxylic Acid Ethyl Ester (**8**).* The title compound was prepared according to the general procedure from indole **7** using 5-(4,4,5,5-tetramethyl-[1,3,2]dioxaborolan-2-yl)-1*H*-indole-2-carboxylic acid ethyl ester **26** (100 mg, 0.31 mmol), 3-bromopyridine (0.03 mL, 0.31 mmol), and bistriphenylphosphine palladium(II) chloride (25 mg, 0.03 mmol) to give the crude product that was purified on reverse-phase HPLC to give the title compound as a white solid (20 mg, 24%). LCMS (ES+) m/z found, 267; retention time, 0.58 min. $C_{16}H_{14}N_2O_2$ requires 267. HPLC retention time, 7.56 min. ^{1}H NMR (400 MHz, DMSO-d_6): δ 12.12 (s, 1H), 9.11 (bs, 1H), 8.71 (bs, 1H), 8.47 (d, J = 7.2 Hz, 1H), 8.10 (s, 1H), 7.60–7.80 (m, 3H), 7.24 (s, 1H), 4.37 (q, J = 3.2 Hz, 2H), 1.36 (t, J = 3.2 Hz, 3H).

*5-Pyridin-4-yl-1H-indole-2-carboxylic Acid Ethyl Ester (**9**).* The title compound was prepared according to the general procedure from indole **7** using 5-(4,4,5,5-tetramethyl-[1,3,2]dioxaborolan-2-yl)-1*H*-indole-2-carboxylic acid ethyl ester **26** (100 mg, 0.31 mmol), 4-bromopyridine hydrochloride (61 mg, 0.31 mmol), and bistriphenylphosphine palladium(II) chloride (25 mg, 0.03 mmol) to give the crude product that was purified on reverse-phase HPLC to give the title compound as a white solid (8 mg, 10%). LCMS (ES+) m/z found, 267; retention time, 0.49 min. $C_{16}H_{14}N_2O_2$ requires 267. HPLC retention time, 7.44 min. ^{1}H NMR (400 MHz, DMSO-d_6): δ 12.25 (s, 1H), 8.81, (d, J = 6.4 Hz, 2H), 8.37 (s, 1H), 8.20 (d, J = 6.4 Hz, 2H), 7.82 (dd, J = 8.4 Hz, 1.6 Hz, 1H), 7.63 (d, J = 8.4 Hz, 1H), 7.29 (d, J = 1.6 Hz, 1H), 4.37 (q, J = 3.2 Hz, 2H), 1.36 (t, J = 3.2 Hz, 3H).

*5-(3-Methyl-pyridin-4-yl)-1H-indole-2-carboxylic Acid Ethyl Ester (**10**).* The title compound was prepared according to the general procedure from indole **7** using 5-(4,4,5,5-tetramethyl-[1,3,2]-dioxaborolan-2-yl)-1*H*-indole-2-carboxylic acid ethyl ester **26** (434 mg, 1.4 mmol), 4-chloro-3-methyl-pyridine hydrochloride (188 mg, 1.4 mmol), bis(di-*tert*-butyl(4-dimethylaminophenyl)phosphine)-dichloropalladium(II) (40 mg, 0.06 mmol), potassium carbonate (965 mg, 6.9 mmol), toluene (4 mL), and water (0.5 mL) to give the crude product that was purified on reverse-phase HPLC to give the

dx.doi.org/10.1021/jm201129m | *J. Med. Chem.* 2011, 54, 8174–8187

title compound as a white solid (50 mg, 15%). LCMS (ES+) m/z found, 281; retention time, 0.54 min. $C_{17}H_{16}N_2O_2$ requires 281. HPLC retention time, 7.96 min. $C_{17}H_{16}N_2O_2$ requires 281. ^{1}H NMR (400 MHz, DMSO-d_6): δ 12.19 (s, 1H), 8.78 (s, 1H), 8.71 (d, J = 5.6 Hz, 1H), 7.86 (s, 1H), 7.78 (d, J = 5.6 Hz, 1H), 7.61 (d, J = 8.8 Hz, 1H), 7.42 (dd, J = 8.8 Hz, 1.6 Hz, 1H), 7.26 (d, J = 1.6 Hz, 1H), 4.37 (q, J = 3.2 Hz, 2H), 2.43 (s, 3H), 1.36 (t, J = 3.2 Hz, 3H).

5-Pyridin-4-yl-1H-indole-2-carboxylic Acid Ethyl Ester (11). The title compound was prepared according to the general procedure from indole **7** using 5-(4,4,5,5-tetramethyl-[1,3,2]dioxaborolan-2-yl)-1*H*-indole-2-carboxylic acid ethyl ester **26** (100 mg, 0.31 mmol), 5-bromo-1-methyl-1*H*-imidazole (51 mg, 0.31 mmol), and bistriphenylphosphine palladium(II) chloride (25 mg, 0.03 mmol) to give the crude product that was purified on reverse-phase HPLC to give the title compound as a white solid (5 mg, 6%). LCMS (ES+) m/z found, 270; retention time, 0.46 min. $C_{15}H_{15}N_3O_2$ requires 270. HPLC retention time, 7.39 min. $C_{15}H_{15}N_3O_2$ requires 270. ^{1}H NMR (400 MHz, DMSO-d_6): δ 12.20 (s, 1H), 9.11 (s, 1H), 7.91 (s, 1H), 7.80 (s, 1H), 7.61 (d, J = 8.8 Hz, 1H), 7.45 (d, J = 8.8 Hz, 1H), 7.25 (s, 1H), 7.36 (q, J = 3.2 Hz, 2H), 3.82 (s, 3H), 1.35 (t, J = 3.2 Hz, 3H).

5-(2-Ethoxycarbonyl-1H-inden-5-yl)-1-methyl-1H-pyrazole-3-carboxylic Acid Methyl Ester (12). But-2-ynedioic acid dimethyl ester (21.6 g, 151 mmol) was added to diethylether (200 mL), and the resulting solution was cooled to −5 °C in a methanol/ice bath. Methylhydrazine (8.1 mL, 151 mmol) in diethyl ether (10 mL) was added dropwise to the solution at a rate such that the internal temperature did not rise above 0 °C. The mixture was stirred for 1 h at −5 °C, and the resulting yellow precipitate was filtered off, washed with ether, and dried in a 40 °C oven. A flask was then charged with the solid, and the flask was immersed in an oil bath heated to 100 °C for 10 min. The solid turned bright orange, and vapor was emitted from the flask. The resulting solid was cooled to room temperature and recrystallized from methanol to give 5-hydroxy-1-methyl-1*H*-pyrazole-3-carboxylic acid methyl ester **27** as a white solid (15 g, 96 mmol).

A sealed tube reaction flask was charged with 5-hydroxy-1-methyl-1*H*-pyrazole-3-carboxylic acid methyl ester (10 g, 64 mmol), phosphorus oxybromide (91 g, 320 mmol), and acetonitrile (200 mL). The flask was sealed and heated to 80 °C for 15 h. Upon completion, the reaction vessel was cooled, and the reaction solution was poured into a precooled solution of saturated sodium bicarbonate. Additional solid sodium bicarbonate was added to the stirred mixture until the solution turned basic. The product was extracted into EtOAc, and the combined organic layers were dried (Na_2SO_4), filtered, and evaporated in vacuo to give 5-bromo-1-methyl-1*H*-pyrazole-3-carboxylic acid methyl ester **28** as a tan solid (6.8 g, 31 mmol, 48%). ^{1}H NMR (400 MHz, DMSO-d_6): δ 6.96 (s, 1H), 3.90 (s, 3H), 3.80 (s, 3H).

The title compound **12** was prepared according to the general procedure from indole **7** using 5-(4,4,5,5-tetramethyl-[1,3,2]-dioxaborolan-2-yl)-1*H*-indole-2-carboxylic acid ethyl ester **26** (113 mg, 0.36 mmol), 5-bromo-1-methyl-1*H*-pyrazole-3-carboxylic acid methyl ester **28** (80 mg, 0.37 mmol), and bistriphenylphosphine palladium(II) chloride (41 mg, 0.06 mmol) to give the crude product that was purified on reverse-phase HPLC to give the title compound **12** as a white solid (14 mg, 13%). LCMS (ES+) m/z found, 328; retention time, 0.85 min. $C_{17}H_{17}N_3O_4$ requires 328. HPLC retention time, 10.53 min. ^{1}H NMR (400 MHz, DMSO-d_6): δ 12.08 (s, 1H), 7.86 (s, 1H), 7.56 (d, J = 8.8 Hz, 1H), 7.42 (dd, J = 8.4 Hz, 1.6 Hz, 1H), 7.21 (d, J = 1.6 Hz), 6.84 (s, 1H), 4.35 (q, J = 3.2 Hz, 2H), 3.91 (s, 3H), 3.80 (s, 3H), 1.34 (t, J = 3.1 Hz, 3H).

5-{2-Methyl-5-[(pyridin-4-ylmethyl)-carbamoyl]-2H-pyrazol-3-yl}-1H-indole-2-carboxylic Acid Ethyl Ester (13). A flask was charged with 5-bromo-1-methyl-1*H*-pyrazole-3-carboxylic acid methyl ester **28** (10 g, 46 mmol) and dioxane (100 mL), and a 4 N solution of lithium hydroxide (57 mL) was added. The reaction was stirred at room temperature for 1 h, then additional water was added, and the organic layer evaporated in vacuo. The water layer was washed twice with dichloromethane and then acidified to pH 2.0 with concentrated HCl. The product was extracted into EtOAc, and the combined organic layers were dried, filtered, and evaporated in vacuo to give 5-bromo-1-methyl-1*H*-pyrazole-3-carboxylic acid **29** (7.1 g, 34 mmol 75%) as a white solid that was used without further purification. ^{1}H NMR (400 MHz, DMSO-d_6): δ 6.87 (s, 1H), 3.89 (s, 3H).

A flask was charged with 5-bromo-1-methyl-1*H*-pyrazole-3-carboxylic acid **29** (500 mg, 2.4 mmol) and HATU (1.1 g, 2.7 mmol). The solids were dissolved in DMF (10 mL), and the reaction was stirred for 1 h at room temperature after which time pyridin-4-yl-methylamine (0.27 mL, 2.7 mmol) and diisopropylethylamine (1.1 mL, 6.1 mmol) were added. The reaction was stirred at room temperature for 24 h and then poured into water, and the product was extracted with EtOAc. The combined organic layers were washed with water and then brine, dried, filtered, and evaporated in vacuo to give 5-bromo-1-methyl-1*H*-pyrazole-3-carboxylic acid (pyridin-4-ylmethyl)-amide **30** (456 mg, 1.5 mmol, 63%) as a solid that was used without further purification.

1*H*-Pyrazole-3-carboxylic acid (pyridin-4-ylmethyl)-amide **30** (100 mg, 0.34 mmol), 5-(4,4,5,5-tetramethyl-[1,3,2]dioxaborolan-2-yl)-1*H*-indole-2-carboxylic acid ethyl ester **26** (113 mg, 0.36 mmol), and bis(di-*tert*-butyl(4-dimethylaminophenyl)phosphine)-dichloropalladium(II) (40 mg, 0.06 mmol) were placed into a microwave vial and suspended in DMF (2 mL), and a 2 M aqueous solution of sodium carbonate (2 mL) was added. The reaction vessel was sealed and heated in a microwave reactor for 20 min at 100 °C. The solution was diluted with EtOAc and filtered though a pad of Celite. The pad was washed with DCM/methanol (1:1), and the combined extracts were washed with water. The organic layer was dried, filtered, and evaporated in vacuo to give an oil that was purified by reverse-phase HPLC to give the title compound **13** (15 mg, 11%). LCMS (ES+) m/z found, 404; retention time, 0.56 min. $C_{17}H_{17}N_3O_4$ requires 404. HPLC retention time, 8.44 min. $C_{17}H_{17}N_3O_4$ requires 404. ^{1}H NMR (400 MHz, DMSO-d_6): δ 12.12 (s, 1H), 9.01 (t, J = 6.0 Hz, 1H), 8.70 (d, J = 5.6 Hz, 2H), 7.87 (s, 1H), 7.67 (d, J = 4.8 Hz, 2H), 7.57 (d, J = 8.4 Hz, 1H), 7.44 (d, J = 8.4 Hz, 1H), 7.23 (s, 1H), 6.77 (s, 1H), 4.59 (d, J = 7.0 Hz, 2H), 4.36 (q, J = 3.2 Hz, 2H), 3.93 (s, 3H), 1.35, (t, J = 3.2 Hz, 3H).

5-{2-Methyl-5-[(6-oxo-1,6-dihydro-pyridin-3-ylmethyl)-carbamoyl]-2H-pyrazol-3-yl}-1H-indole-2-carboxylic Acid Ethyl Ester (14). The title compound was prepared according to the procedure described for **13** from 5-bromo-1-methyl-1*H*-pyrazole-3-carboxylic acid **29** (200 mg, 0.97 mmol), HATU (371 mg, 0.97 mmol), 5-aminoethyl-1*H*-pyridin-2-one (121 mg, 0.97 mmol), DMF (1 mL), and diisopropyethylamine (0.18 mL, 0.97 mmol) to give the amide **14** (200 mg, 66%). LCMS (ES+) m/z found, 420; retention time, 0.66 min. $C_{22}H_{21}N_5O_4$ requires 420. HPLC retention time, 9.07 min. ^{1}H NMR (400 MHz, DMSO-d_6): δ 12.06 (brd, 1H), 11.42 (brd, 1H), 8.56 (t, J = 6.4 Hz, 1H), 7.84 (s, 1H), 7.56 (d, J = 8.8 Hz, 1H), 7.44 (dd, J = 9.2 Hz, 2.4 Hz, 1H), 7.41 (dd, J = 8.4 Hz, 1.6 Hz, 1H), 7.24 (d, J = 2.4 Hz, 1H), 7.21 (s, 1H), 6.71 (s, 1H), 6.29 (d, J = 9.2 Hz, 1H), 4.35 (q, J = 3.2 Hz, 2H), 4.14 (d, J = 7.0 Hz, 2H), 3.88 (s, 1H), 1.34 (s, J = 3.2 Hz, 3H).

5-[5-(4-Carboxy-benzylcarbamoyl)-2-methyl-2H-pyrazol-3-yl]-1H-indole-2-carboxylic Acid Ethyl Ester (15). A flask is charged with 5-bromo-1-methyl-1*H*-pyrazole-3-carboxylic acid **29** (7.25 g 35 mmol), TBTU (14.7 g, 38 mmol), and DMF (50 mL), and the reaction was stirred for 30 min. 4-Aminomethyl-benzoic acid methyl ester hydrochloride (7.84 g, 38 mmol) was added followed by Hunnings base (16.2 mL, 88 mmol), and the reaction was sealed and stirred overnight for24 h. The reaction was poured into water and extracted into EtOAc. The organic layer was washed with water, saturated sodium bicarbonate, and brine, dried, filtered, and evaporated in vacuo to give 4-{[(5-bromo-1-methyl-1*H*-pyrazole-3-carbonyl)-amino]-methyl}-benzoic acid methyl ester **32**, which was used directly without further purification.

The above ester **32** (2.0 g, 5.6 mmol) was dissolved in 1,4-dioxane (30 mL), and 4 N warm lithium hydroxide (5.67 mL, 22 mmol) was added to the solution. The reaction was stirred at room temperature for 1 h, then water was added, and then, the organic layer was evaporated in vacuo. The water layer was washed with dichloromethane and acidified to pH 2 with concentrated HCl. The reaction was evaporated to 50% volume, and the resulting solid was collected,

washed with 1 N HCl, and dried in vacuo to give 4-{[(5-bromo-1-methyl-1*H*-pyrazole-3-carbonyl)-amino]-methyl}-benzoic acid **33** (1.9 g, 93%). ^{1}H NMR (400 MHz, DMSO-d_6): δ 12.78 (bs, 1H), 8.83 (t, J = 6.4 Hz, 1H), 7.87 (d, J = 8.4 Hz, 2H), 7.37 (d, J = 8.0 Hz, 2H), 6.82 (s, 1H), 4.47 (d, J = 6.4 Hz, 2H), 3.88 (s, 3H).

A reaction flask was charged with 4-{[(5-bromo-1-methyl-1*H*-pyrazole-3-carbonyl)-amino]-methyl}-benzoic acid **33** (7.0 g, 20 mmol), 5-(4,4,5,5-tetramethyl-[1,3,2]dioxaborolan-2-yl)-1*H*-indole-2-carboxylic acid ethyl ester **26** (6.5 g, 20 mmol), tetrakistriphenyphosphine palladium(0) (2.9 g, 2.5 mmol) THF (600 mL), and 2 M aqueous solution of sodium bicarbaonate (60 mL, 120 mmol). The mixture was heated to reflux for 24 h and cooled to room temperature, and the solvent was evaporated in vacuo. The crude material was partitioned between water and EtOAc, and the aqueous layer was isolated and acidified to pH 3 with concentrated HCl. The resulting precipitate was collected by filtration and purified on silica (methanol/dichloromethane) to give the title compound **15** as a white solid. LCMS (ES+) m/z found, 447; retention time, 0.80 min. $C_{24}H_{22}N_4O_5$ requires 447. HPLC retention time, 10.12 min. ^{1}H NMR (400 MHz, DMSO-d_6): δ 12.12 (s, 1H), 8.80 (t, J = 6.4 Hz, 1H), 7.89 (s, 1H), 7.87 (s, 2H), 7.57 (d, J = 8.4 Hz, 1H), 7.43 (dd, J = 8.4 Hz, 1.6 Hz, 1H), 7.36 (d, J = 8.4 Hz, 2H), 7.22 (d, J = 1.6 Hz, 1H), 6.75 (s, 1H), 4.48 (d, J = 6.0 Hz, 2H), 4.35 (q, J = 3.2 Hz, 2H), 3.91 (s, 3H), 1.35 (t, J = 3.2 Hz, 3H).

*5-[5-(4-Carboxymethyl-benzylcarbamoyl)-2-methyl-2H-pyrazol-3-yl]-1H-indole-2-carboxylic Acid Ethyl Ester (**16**).* A flask was charged with 5-bromo-1-methyl-1*H*-pyrazole-3-carboxylic acid **29** (250 mg, 1.2 mmol), HATU (463 mg, 1.2 mmol), and DMF (2 mL), and the reaction was stirred for 30 min. (4-Aminomethyl-phenyl)-acetic acid methyl ester hydrochloride (260 mg, 1.2 mmol) was added followed by DIEA (0.45 mL, 2.4 mmol), and the reaction was sealed and stirred overnight for 24 h. The solvents were evaporated in vacuo, and the crude material was partitioned between EtOAc and water. The organic layer was washed thrice with water, dried over magnesium sulfate, filtered, and evaporated in vacuo to give an oil that was purified on silica (EtOAc/heptanes) to give (4-{[(5-bromo-1-methyl-1*H*-pyrazole-3-carbonyl)-amino]-methyl}-phenyl)-acetic acid methyl ester **34** (330 mg, 74%).

The above ester **34** (150 mg, 0.4 mmol) was dissolved in THF (2.5 mL) and water (1.0 mL), and lithium hydroxide monohydrate (50 mg, 2.0 mmol) was added to the solution. The reaction was stirred at room temperature for 24 h and then quenched with concentrated HCl to a pH of 2.0. The solvent was evaporated in vacuo, and the solids were diluted with water and EtOAc. The product was extracted into EtOAc, and the organic layer was dried ($MgSO_4$), filtered, and evaporated in vacuo to give a white solid **25** that was used with out further purification (140 mg, 97%). ^{1}H NMR (400 MHz, DMSO-d_6): δ 12.23 (s, 1H), 8.69 (t, J = 6.4 Hz, 1H), 7.19 (q, J = 8.0 Hz, 4H), 6.80 (s, 1H), 4.36 (d, J = 6.4 Hz, 2H), 3.87 (s, 3H), 3.50 (s, 2H).

A reaction flask was charged with (4-{[(5-bromo-1-methyl-1*H*-pyrazole-3-carbonyl)-amino]-methyl}-phenyl)-acetic acid **35** (100 mg, 0.28 mmol), 5-(4,4,5,5-tetramethyl-[1,3,2]dioxaborolan-2-yl)-1*H*-indole-2-carboxylic acid ethyl ester **26** (90 mg, 0.28 mmol), tetrakistrkistriphenyphosine palladium(0) (10 mg, 0.03 mmol), THF (5 mL), and 2 M aqueous sodium bicarbonate (0.75 mL). The mixture was heated to reflux for 24 h and cooled to room temperature, and the solvent was evaporated in vacuo. The crude material was partitioned between water and EtOAc, and the aqueous layer was isolated and acidified to pH 3 with concentrated HCl. The resulting precipitate was collected by filtration and purified by reverse-phase HPLC to give a white solid (14 mg, 11%). LCMS (ES+) m/z found, 461; retention time, 0.80 min. $C_{25}H_{24}N_4O_5$ requires 461. HPLC retention time, 10.15 min. ^{1}H NMR (400 MHz, DMSO-d_6): δ 12.29 (s, 1H), 12,11 (s, 1H), 8.69 (t, J = 6.0 Hz, 1H), 7.86 (s, 1H), 7.56 (d, J = 8.8 Hz, 1H), 7.43 (dd, J = 8.8 Hz, 1.6 Hz, 1H), 7.24 (d, J = 8 Hz, 2H), 7.22 (d, J = 1.6 Hz, 1H), 7.19 (d, J = 8.4 Hz, 2H),6.73 (s, 1H), 4.40 (d, J = 6.0 Hz, 2H), 4.35 (q, J = 3.2 Hz, 2H), 3.90 (s, 3H), 3.52 (s, 2H), 1.35 (t, J = 3.2 Hz, 3H).

*5-{5-Methyl-2-[(pyridin-4-ylmethyl)-carbamoyl]-pyridin-4-yl}-1H-indole-2-carboxylic Acid Ethyl Ester (**17**).* A microwave reaction flask was charged with 5-(4,4,5,5-tetramethyl-[1,3,2]dioxaborolan-2-yl)-1H-indole-2-carboxylic acid ethyl ester **26** (510 mg, 1.6 mmol), 4-Chloro-5-methyl-pyridine-2-carboxylic acid (300 mg, 1.61 mmol), bis(di-t-butylphosphino (4-dimethylaminophenyl)) palladium(II)dichloride (230 mg, 0.32 mmol), and the solids suspended in DMF (6 mL) and 2N sodium carbonate (2 mL). The reaction vessel was sealed and heated to 100 °C for 20 min in a microwave reactor. The reaction was cooled to room temperature, filtered through Celite, and washed with EtOAc and ammonium hydroxide. The aqueous layer was separated, and acidified with concentrated HCl. The solvent was removed in vacuo and the crude material **37** used without further purification.

5-(2-Carboxy-5-methyl-pyridin-4-yl)-1*H*-indole-2-carboxylic acid ethyl ester **37** (15 mg, 0.05 mmol) was dissolved in DMF (1 mL), and HATU (26 mg, 0.07 mmol) and DIEA (0.03 mL 0.07 mmol) were added. The reaction was stirred for 30 min, then C-pyridin-4-yl-methylamine (8 μL, 0.07 mmol) was added to the reaction, and the resulting mixture was stirred at room temperature overnight. The solvents were evaporated in vacuo, and the crude product was purified directly by reverse-phase HPLC to give the title compound **17** as a white solid (10 mg, 52%) LCMS (ES+) m/z found, 415; retention time, 0.67 min. $C_{24}H_{22}N_4O_3$ requires 415. HPLC retention time, 9.20 min. ^{1}H NMR (400 MHz, DMSO-d_6): δ 12.08 (s, 1H), 9.50 (t, J = 6.4 Hz, 1H), 8.61 (s, 1H), 8.50 (d, J = 4.8 Hz, 2H), 7.90 (s, 1H), 7.77 (s, 1H), 7.57 (d, J = 8.4 Hz, 1H), 7.36 (d, J = 8.4 Hz, 1H), 7.31 (d, J = 4.8 Hz, 2H), 7.23 (s, 1H), 4.52 (s, 2H), 4.36 (q, J = 3.2 Hz, 2H), 2.38 (s, 3H), 1.35 (t, J = 3.2 Hz, 3H).

*5-[5-(4-Carboxy-benzylcarbamoyl)-2-methyl-2H-pyrazol-3-yl]-1H-indole-2-carboxylic (**18**).* A flask was charged with 5-[5-(4-carboxy-benzylcarbamoyl)-2-methyl-2*H*-pyrazol-3-yl]-1*H*-indole-2-carboxylic acid ethyl ester **15** (35 mg, 0.08 mmol) and taken up in 1,4-dioxane (1 mL), and lithium hydroxide in water (4 N, 0.1 mL) was added. The reaction was stirred for 3 h and then acidified to pH 2 with concentrated HCl. The reaction flask was cooled to 0 °C, and the resulting precipitate was collected, washed with ice cooled water, and dried in vacuo to give the title compound (15 mg, 45%). LCMS (ES+) m/z found, 419; retention time, 0.61 min. $C_{21}H_{18}N_4O_5$ requires 419. HPLC retention time, 8.29 min. ^{1}H NMR (400 MHz, DMSO-d_6): δ 13.06 (bs, 1H), 12.85 (b, 1H), 11.97 (s, 1H), 8.81 (t, J = 6.4 Hz, 1H), 7.89 (d, J = 8.0 Hz, 2H), 7.84 (s, 1H), 7.54 (d, J = 8.4 Hz, 1H), 7.42–7.39 (m, 3H), 7.15 (d, J = 1.6 Hz, 1H), 6.73 (s, 1H), 4.49 (d, J = 6.0 Hz, 2H), 3.91 (s, 3H).

*4-({[5-(1H-indol-5-yl)-1-methyl-1H-pyrazole-3-carbonyl]-amino}-methyl)-bezoic Acid (**19**).* A reaction flask was charged with 4-{[(5-bromo-1-methyl-1*H*-pyrazole-3-carbonyl)-amino]-methyl}-benzoic acid **33** (75 m g, 0.22 mmol, from example 14), 5-indoleboronic acid (40 mg, 0.24 mmol), and tetrakistriphenyphosphine palladium(0) (9 mg, 0.003 mmol), and the solids were taken up in THF (4 mL). The reaction was heated to reflux for 24 h, cooled to room temperature, and diluted with EtOAc and water. The aqueous layer was separated and acidified to pH 2 with concentrated HCl, and the resulting solid was collected and purified by reverse-phase HPLC to give the title compound **19** (20 mg, 24%). LCMS (ES+) m/z found, 375; retention time, 0.70 min. $C_{21}H_{18}N_4O_3$ requires 375. HPLC retention time, 9.20 min. $C_{21}H_{18}N_4O_3$ requires 375. ^{1}H NMR (400 MHz, DMSO-d_6): δ 12.86 (s, 1H), 11.31 (s, 1H), 8.82 (t, J = 6.4 Hz, 1H), 7.89 (d, J = 8.4 Hz, 2H), 7.72 (s, 1H), 7.51 (d, J = 8.4 Hz, 1H), 7.44 (t, J = 2.8 Hz, 1H), 7.41 (d, J = 8.0 Hz, 2H), 7.23 (dd, J = 8.4 Hz, 1.6 Hz, 1H), 6.70 (s, 1H), 6.51 (m, 1H), 4.49, (d, J = 6.4 Hz, 2H), 3.91 (s, 3H).

*4-({[5-(20-Ethoxymethyl-1H-indol-5-yl)-1-methyl-1H-pyrazole-3-carbonyl]-amino}-methyl)-bezoic Acid (**20**).* A flask was charged with 5-bromo-1*H*-indole-2-carboxylic acid ethyl ester **25** (4.5 g, 16 mmol) and THF (50 mL), and the reaction cooled to 0 °C in an ice bath. Sodium hydride (60% in mineral oil, 740 mg, 18 mmol) was added portion wise to the reaction over 10 min, and the resulting slurry was stirred for 15 min, and then, 2-(trimethylsilyl)ethoxymethyl chloride (SEM-Cl) (3.2 mL, 18 mmol) was added to the reaction. The reaction was stirred at 0 °C for 4 h and then quenched by the addition of water, and the product was extracted into diethyl ether. The organic layers were combined, dried over sodium sulfate, filtered, and evaporated in vacuo to give an oil that was purified on silica

(hexanes/EtOAc) to give 5-bromo-1-(2-trimethylsilanyl-ethoxymethyl)-1*H*-indole-2-carboxylic acid ethyl ester **38** as a clear oil. ^{1}H NMR (400 MHz, DMSO-d_6): δ 7.94 (d, J = 2.0 Hz, 1H), 7.68 (d, J = 8.8 Hz, 1H), 7.49 (dd, J = 8.8 Hz, 2.0 Hz, 1H), 7.32 (s, 1H), 5.94 (s, 2H), 4.32 (q, J = 7.2 Hz, 2H), 3.41 (t, J = 8.0 Hz, 2H), 1.32 (t, J = 7.2 Hz, 3H), 0.75 (t, J = 8.0 Hz, 2H), 0.14 (s, 9H).

The above ester **38** (5.1 g, 12 mmol) was placed into a flask and dissolved in THF (40 mL) and ether (40 mL). The flask was cooled to 0 °C, and $LiAlH_4$ (1.0 g, 25 mmol) was added portion wise to the reaction (Caution: hydrogen gas evolution) under argon. The resulting slurry was stirred for 1.5 h at 0 °C and then quenched by the addition of 1 mL of water, 1 mL of 15% aqueous sodium hydroxide, and 3 mL of water to give a suspension that is filtered, and the filtrate was evaporated in vacuo to give [5-bromo-1-(2-trimethylsilanyl-ethoxymethyl)-1*H*-indol-2-yl]-methanol **39** as an oil that was used without further purification.

A flask was charged with the above indole **39** (500 mg, 1.4 mmol), silver(II) oxide (1 g, 4.2 mmol), ethyl iodide (1.6 mL, 14 mmol), and acetonitrile (5 mL). The reaction was stirred at room temperature for 4 h and then heated to 50 °C for 16 h. After it was cooled, the reaction was passed though Celite and evaporated in vacuo to give an oil that was purified on silica (hexanes/EtOAc) to give 5-bromo-2-ethoxymethyl-1-(2-trimethylsilanyl-ethoxymethyl)-1*H*-indole **40** as a clear oil (238 mg, 50%). ^{1}H NMR (400 MHz, DMSO-d_6): δ 7.72 (d, J = 2.0 Hz, 1H), 7.53 (d, J = 8.4 Hz, 1H), 7.28 (dd, J = 8.8 Hz, 2.0 Hz, 1H), 6.50 (s, 1H), 5.55 (s, 2H), 4.64 (s, 2H), 3.49 (q, J = 7.2 Hz, 2H), 3.46 (t, J = 8.0 Hz, 2H), 1.13 (t, J = 7.2 Hz, 3H), 0.79 (t, J = 8.0 Hz, 2H), 0.10 (s, 9H).

A flask was charged with 5-bromo-2-ethoxymethyl-1-(2-trimethylsilanyl-ethoxymethyl)-1*H*-indole **40** (500 mg, 1.3 mmol), potassium carbonate (380 mg, 3.9 mmol), ditetramethylenediborane (360 mg, 1.4 mmol), and bis-diphenylferrocenylpalladium(II) dichloride (210 mg, 0.3 mmol), and the solids were suspended in 1,4-dioxane (10 mL) and DMF (7 mL). The reaction was sealed and heated to 100 °C for 1 h and then cooled to room temperature. The solution was diluted with EtOAc and washed with water. The organic layer was dried filtered, evaporated in vacuo, and purified on silica (heptanes/EtOAc) to give 2-ethoxymethyl-5-(4,4,5,5-tetramethyl-[1,3,2]dioxaborolan-2-yl)-1-(2-trimethylsilanyl-thoxymethyl)-1*H*-indole **41** as a white solid (350 mg, 62%). ^{1}H NMR (400 MHz, DMSO-d_6): δ 7.91 (s, 1H), 7.54 (d, J = 8.4 Hz, 1H), 7.46 (d, J = 8.0 Hz, 1H), 6.54 (s, 1H), 5.56 (s, 2H), 4.64 (s, 2H), 3.50 (q, J = 7.2 Hz, 2H), 3.45 (t, J = 8.4 Hz, 2H), 1.29 (s, 12H), 1.14 (t, J = 7.2 Hz, 3H), 0.80 (t, J = 8.0 Hz, 2H), 0.10 (s, 9H).

A reaction flask was charged with the boronic acid **41** from above (185 mg, 0.4 mmol), 4-{[(5-bromo-1-methyl-1H-pyrazole-3-carbonyl)-amino]-methyl}-benzoic acid **33** (120 mg, 0.33 mmol, from example **14**), and tetrakistrkistriphenyphosine palladium(0) (32 mg, 0.03 mmol), the solids were suspended in THF (3 mL), and 2 N aqueous sodium carbonate (0.75 mL) was added. The reaction was heated for 6 h at reflux and then cooled to room temperature, and the solvent evaporated in vacuo. The resulting oil was taken up in EtOAc/water and acidified to pH 2 with concentrated HCl. The product was then extracted into copious amounts of ethyl acetate. The combined organic layers were dried ($MgSO_4$), filtered, and evaporated in vacuo to give an oil that was purified on silica (MeOH/DCM) to give a solid **42** (150 mg, 75%). ^{1}H NMR (400 MHz, DMSO-d_6): δ 8.81 (t, J = 6.4 Hz, 1H), 7.89 (d, J = 8.0 Hz, 2H), 7.72 (d, J = 1.6 Hz, 1H), 7.69 (d, J = 8.8 Hz, 1H), 7.37 (d, J = 8.0 Hz, 2H), 7.34 (dd, J = 8.4 Hz, 1.6 Hz, 1H), 6.73 (s, 1H), 6.60 (s, 1H), 5.61 (s, 2H), 4.68 (s, 2H), 4.49 (d, J = 6.4 Hz, 2H), 3.91 (s, 3H), 3.46–3.54 (m, 4H), 1.15 (t, J = 7.2 Hz, 3H), 0.82 (t, J = 8.0 Hz, 2H), 0.08 (s, 9H).

A flask was charged with 4-[({5-[2-ethoxymethyl-1-(2-trimethylsilanyl-ethoxymethyl)-1*H*-indol-5-yl]-1-methyl-1*H*-pyrazole-3-carbonyl}-amino)-methyl]-benzoic acid **42** (25 mg, 0.04 mmol), THF (1 mL), and ethylenediame (10 μL, 0.13 mmol), and tetrabutlyammonium fluoride (0.25 mL, 1 M in THF) was added dropwise to the reaction. The reaction was heated to 70 °C for 5 h, then cooled to room temperature, and evaporated in vacuo to give a solid that was purified directly on reverse-phase HPLC to give the title compound **20** as a white solid (6 mg, 31%). LCMS (ES+) m/z found, 433; retention time, 0.78 min. $C_{24}H_{24}N_4O_4$ requires 433. HPLC retention time, 9.82 min. ^{1}H NMR (400 MHz, DMSO-d_6): δ 12.85 (brd, 1H), 11.37 (s, 1H), 8.81 (t, J = 6.4 Hz, 1H), 7.89 (d, J = 8.4 Hz, 2H), 7.65 (s, 1H), 7.44 (d, J = 8.4 Hz, 1H), 7.40 (d, J = 8.4 Hz, 2H), 7.20 (dd, J = 8.4 Hz, 1.6 Hz, 1H), 6.67 (s, 1H), 6.43 (s, 1H), 4.58 (s, 2H), 4.49 (d, J = 6.4 Hz, 2H), 3.89 (s, 3H), 3.49 (q, J = 6.8 Hz, 2H), 1.14 (t, J = 6.8 Hz, 3H).

Crystallography. A fragment of human MMP-13 corresponding to residues 104–274 was expressed using the pET29a vector system (Invitrogen) and *E. coli* BL21(DE3) host strain. The protein was expressed in insoluble form. Cell pellets were lysed at 4 °C using five, 1 min cycles of sonication in a buffer containing 50 mM MES, 75 mM NaCl, and 0.5% Triton at pH 6.5. Following sonication, the pellet was recovered by centrifugation, and the supernatant was decanted. This sonication process was repeated three times, with the final pellet, containing the inclusion bodies, being frozen at −80 °C. The pellet containing the inclusion bodies was thawed and resolubilized at room temperature in a buffer containing 6 M urea and 150 mM MES, pH 6.5. Inhibition of protease activity was achieved through the addition of Complete protease inhibitor cocktails (Roche). The resuspended material was clarified using centrifugation, and the supernatant was recovered. The supernatant was dialyzed against a buffer containing 6 M urea and 50 mM MES, pH 6.5. The dialyzed material was then purified using an SP Sepharose Fast Flow resin (GE LifeSciences). Separation was achieved using a buffer containing 6 M urea and 50 mM MES, pH 6.5, and a gradient of 0–250 mM NaCl. Fractions containing the MMP-13 were pooled and stored at −80 °C.

The protein was refolded using sequential dialysis of the protein (at a concentration of 0.25 mg/mL) against a buffer containing 50 mM MES, pH 6.5, 500 mM NaCl, 10 mM $CaCl_2$, 1.0 mM $ZnCl_2$, and urea. The concentration of urea was reduced in the following steps: 4, 2, 1, 0, and 0 M, over the course of approximately 2 days. The dialyzed protein was then concentrated to ∼13 mg/mL, and purification and buffer exchange was achieved via SEC on a Superdex75 resin (GE LifeSciences) with a running buffer of 50 mM Tris, pH 8.0, 150 mM NaCl, and 5 mM $CaCl_2$. The fractions corresponding to MMP-13 were pooled and concentrated to 7 mg/mL.

A 2-fold excess of compound **1** was added to the protein, and crystals were obtained using a hanging drop procedure with a precipitant containing 10% w/v PEG4000, 1 M ammonium formate, and 100 mM Tris, pH 8.0. Crystals with compounds **11** and **15** were obtained by soaking out of crystals containing compound **1**.

X-ray diffraction data were collected using either a Rigaku FR-E SuperBright generator and Saturn92 CCD detector or the PX1 beamline at the SwissLight Source. Data reduction was achieved using HKL2000. An initial structure was obtained via molecular replacement using published coordinates of MMP-13 (PDB: 1XUD) as a starting model. Multiple rounds of refinement were performed using Phenix. The costructure of MMP-13 with compound **1** had a resolution of 1.85 Å and R/R_{free} statistics of 0.17/0.23. The costructure of MMP-13 with compound **15** had a resolution of 2.03 Å and R/R_{free} statistics of 0.16/0.19. The costructure of MMP-13 with compound **11** had a resolution of 1.79 Å and R/R_{free} statistics of 0.24/0.28.

Biological Assays. Catalytic domains of human MMP-13 were expressed and purified from *E. coli* in house. MMP-13 was assayed in a 20 μL volume containing a 125 pM catalytic domain of human MMP-13 and 2 μM 520 MMP FRET Substrate XIV [sequence: QXL520-GABA-Pro-Cha-Abu-Smc-His-Ala-Dab(5-FAM)-Ala_Lys-NH_2] (Anaspec) in a buffer containing 100 mM Tris HCl, pH 7.5, 100 mM NaCl, 10 mM $CaCl_2$, and 0.05% BRIJ 35, and 1% DMSO for 30 min at 28 °C/80% humidity, and fluoresence was read at 485 nm excitation and 535 nm emission. All other MMPs were assayed as described for MMP-13 with enzyme substitutions as follows: 4 nM catalytic domain of recombinant human MMP-1(Biomol), 2 nM catalytic domain of recombinant human MMP-2 (Biomol), 0.8 nM catalytic domain of recombinant human MMP-3 (Biomol), 0.6 nM catalytic domain of recombinant human MMP-7 (Biomol), 2 nM catalytic domain of recombinant human MMP-8 (Biomol), 1.5 nM catalytic domain of recombinant human MMP-9 (Biomol), 1 nM catalytic domain of recombinant human MMP-10 (Biomol), and 0.125 nM catalytic

domain of recombinant human MMP-12 (Biomol). MMP-14 was assayed as described for MMP-13 with an enzyme substitution of 8.8 nM catalytic domain of recombinant human MMP-14 (Biomol) and an extended linear incubation time of 60 min at 28 °C/80% humidity. MMP-13 with 1.25% human serum was assayed as described for MMP-13 with the addition of 1.25% human serum to the assay buffer.

For the collagen degradation assay (MMP-13 IC_{50} full length), the Rapid Collagen Assay kit by Condrex (catalog #3002) was applied to measure the activity of MMP-13 in degrading FITC labeled collagen II. Full-length MMP-13 was activated by 1 mM AMPA, and the activated FL-MMP13 (600 ng/mL) was incubated with FITC-labeled type II collagen in the kit assay buffer for 1.5 h at 37 °C. The degraded collagen fragments were extracted into solution and measured by fluorescent intensity of FITC (490 nm ex/520 nm em) as described in the assay kit protocol (www.chondrex.com/protocols/Collagenase_Kit.pdf). IC_{50} values are determined by nonlinear curve fitting of the data from a duplicate 10-point concentration−response curve.

The bovine nasal cartilage (BNC) degradation assay measures the ability of compounds to inhibit full-length MMP-13-induced cartilage degradation. BNC explants were purchased from Northland Laboratories (www.northlandlabs.com) as 3 mm explants in 96-well plates. The BNC explants were washed with PBS and cultured with activated full-length human MMP-13 (50 μg/mL) (BioMol) in the assay buffer containing 50 mM Tris, pH 6.5, 250 mM NaCl, 5 mM $CaCl_2$, 1 μM $ZnCl_2$, and 10% human serum for 2 h at 37 °C. The cartilage degradation products C-terminal telopeptide of type II collagen (CTXII) were quantified by an CTXII ELISA (IDS, formerly Nordic Bioscience, catalog #3CAL4000) using the cartilage culture supernatants. Test compound EC_{50} values are determined by nonlinear curve fitting of the data from duplicate 8-point concentration−response curve.

■ ASSOCIATED CONTENT

Ⓢ Supporting Information

In-depth procedures for target independent assays. This material is available free of charge via the Internet at http://pubs.acs.org.

■ AUTHOR INFORMATION

Corresponding Author

*Tel: 203-791-6371. E-mail: steven.taylor@boehringer-ingelheim.com.

■ ACKNOWLEDGMENTS

The authors thank Kathleen Haverty, Alistair Baptiste and Xiang Zhu for expression and purification of the human MMP-13 catalytic domain.

■ ABBREVIATIONS USED

MMP, matrix metalloproteases; HTS, high-throughput screening; ALI, alternative lead identification; FBS, fragment-based screening; MW, molecular weight; AMU, atomic mass units; clog *P*, calculated partion coefficient in octanol:water; NMR, nuclear magnetic resonance; SPR, surface plasmon resonance; MSS, muscular skeletal syndrome; STD-NMR, saturation transfer difference nuclear magnetic resonance; SEC-MS, size exclusion chromatography mass spectrometry; HBA, hydrogen bond acceptor; HBD, hydrogen bond donor; LE, ligand efficiency $RT\ \ln(IC_{50})$/no. of heavy atoms; PAMPA, parallel artificial membrane permeability assay; PSA, polar surface area; DMF, dimethylformamide; HATU, 2-(1*H*-7-azabenzotriazol-1-yl)-1,1,3,3-tetramethyl uronium hexafluorophosphate methanaminium; TBTU, *O*-(benzotriazol-1-yl)-*N*,*N*,*N*′,*N*′-tetramethyluronium tetrafluoroborate; DIEA, *N*,*N*-diisopropylethylamine; THF, tetrahydrofuran; DBU, 1,8-diazabicyclo[5.4.0]undec-7-ene; SEM-Cl, 2-(trimethylsilyl)ethoxymethyl chloride; TBAF, tetra-*n*-butylammonium fluoride; HPLC, high performance liquid chromatography; BNC, bovine nasal cartilage; h/r LM, human/rat liver microsome stability

■ REFERENCES

(1) Eitner, K.; Koch, U. From fragment screening to potent binders: strategies for fragment-to-lead evolution. *Mini Rev. Med. Chem.* **2009**, *9*, 956−961. (b) Schulz, M. N.; Hubbard, R. E. Recent progress in fragment-based lead discovery. *Curr. Opin. Pharmacol.* **2009**, *9*, 615−621. (c) Mayr, L. M.; Bojanic, D. Novel trends in high-throughput screening. *Curr. Opin. Pharmacol.* **2009**, *9*, 580−5888.

(2) Bembenek, S. D.; Tounge, B. A.; Reynolds, C. H. Ligand efficiency and fragment-based drug discovery. *Drug Discovery Today* **2009**, *14*, 278−283.

(3) Jacoby, E.; Davies, J.; Blommers, M. J. Design of small molecule libraries for NMR screening and other applications in drug discovery. *Curr. Top. Med. Chem.* **2003**, *3*, 11−23.

(4) (a) Shuker, S. B.; Hajduk, P. J.; Meadows, R. P.; Fesik, S. W. Discovering high-affinity ligands for proteins: SAR by NMR. *Science* **1996**, *274*, 1531−1542. (b) Hajduk, P. J.; Sheppard, G.; Nettesheim, D. G.; Olejniczak, E. T.; Shuker, S. B.; Meadows, R. P.; Steinman, D. H.; Carrera, G. M. Jr.; Marcotte, P. A; Severin, J.; Walter, K.; Smith, H.; Gubbins, E.; Simmer, R.; Holzman, T. F.; Morgan, D. W.; Davidsen, S. K.; Summers, J. B.; Fesik, S. W. Discovery of potent nonpeptide inhibitors of stromelysinusing SAR by NMR. *J. Am. Chem. Soc.* **1997**, *119*, 5818−5827. (c) Fejzo, J.; Lepre, C. A.; Peng, J. W.; Bemis, G. W.; Murcko, M. A.; Moore, J. M. The SHAPES strategy: An NMR-based approach for lead generation in drug discovery. *Chem. Biol.* **1999**, *6*, 755−769.

(5) Neumann, T.; Junker, H. D.; Schmidt, K.; Sekul, R. SPR-based fragment screening: Advantages and applications. *Curr. Top. Med. Chem.* **2007**, *7*, 1630−1642.

(6) Recht, M. I.; De Bruyker, D.; Bell, A. G.; Wolkin, M. V.; Peeters, E.; Anderson, G. B.; Kolatkar, A. R.; Bern, M. W.; Kuhn, P.; Bruce, R. H.; Torres, F. E. Enthalpy array analysis of enzymatic and binding reactions. *Anal. Biochem.* **2008**, *377*, 33−39.

(7) (a) Alex, A. A.; Flocco, M. M. Fragment Based Drug Discovery. *Drug Discovery Today* **2009**, *13*−*14*, 668−675. (b) Chessari, G.; Woodhead, A. J. From fragment to clinical candidate—A historical perspective. *Curr. Top. Med. Chem.* **2007**, *7*, 1544−1567.

(8) (a) Morrison, C. J.; Butler, G. S.; Rodríguez, D.; Overall, C. M. Matrix metalloproteinase proteomics: substrates, targets, and therapy. *Curr. Opin. Cell Biol.* **2009**, *5*, 645−653. (b) Cudic, M.; Fields, G. B. Extracellular proteases as targets for drug development. *Curr. Protein Pept. Sci.* **2009**, *4*, 297−307. (c) Tu, G.; Xu, W.; Huang, H.; Li, S. Progress in the development of matrix metalloproteinase inhibitors. *Curr. Med. Chem.* **2008**, *15*, 1388−1395. (d) Fingleton, B. Matrix metalloproteinases as valid clinical targets. *Curr. Pharm. Des.* **2007**, *13*, 333−346. (e) Li, X.; Li, J. Recent advances in the development of MMPIs and APNIs based on the pyrrolidine platforms. *Mini Rev. Med. Chem.* **2010**, *9*, 794−805. (f) Woessner, J. F., Nagase, H., Eds. *Matrix Metalloproteinases and TIMPs*; Oxford University Press: New York, 2000; pp 1−240.

(9) Historically, MMP-1 and -14 were the postulated key players in causing MSS. However, the nonselective MMP-13 inhibitor CP-544439, which is inactive against MMP-1, has caused MSS in clinical trials: Reiter, L. A.; Freeman-Cook, K. D.; Jones, C. S.; Martinelli, G. J.; Antipas, A. S.; Berliner, M. A.; Datta, K.; Downs, J.; Eskra, J. D.; Forman, M. D.; Greer, E. M.; Guzman, R.; Hardink, J. R.; Janat, F.; Keene, N. F.; Laird, E. R.; Liras, J.; Lopresti-Morrow, L. L.; Mitchell, P. G.; Pandit, J.; Robertson, D.; Sperger, D.; Vaughn-Bowser, M. L.; Waller, D. M.; Yocum, S. A. Potent, selective pyrimidinetrione-based inhibitors of MMP-13. *Bioorg. Med. Chem. Lett.* **2006**, 5822−5826. MMP-14 has KO mice data supporting it being a strong candidate for MSS Rowan, A. D.; Litherland, G. J.; Hui, W.; Milner, J. M. Metalloproteases as potential therapeutic targets in arthritis treatment. *Expert Opin. Ther. Targets* **2008**, *12*, 1−18, and references therein..

(10) Vincenti, M. P.; Brinckerhoff, C. E. Transcriptional regulation of collagenase (MMP-1, MMP-13) genes in arthritis: Integration of complex signaling pathways for the recruitment of gene-specific transcription factors. *Arthritis Res.* **2002**, *4*, 157−164.
(11) Tallant, C.; Marrero, A.; Gomis-Rüth, F. X. Matrix metalloproteinases: Fold and function of their catalytic domains. *Biochim. Biophys. Acta* **2010**, *1*, 20−28.
(12) (a) Jacobsen, J. A.; Major Jourden, J. L.; Miller, M. T.; Cohen, S. M. To bind zinc or not to bind zinc: an examination of innovative approaches to improved metalloproteinase inhibition. *Biochim. Biophys. Acta* **2010**, *1*, 72−94. (b) Nuti, E.; Tuccinardi, T.; Rossello, A. Matrix metalloproteinase inhibitors: new challenges in the era of post broad-spectrum inhibitors. *Curr. Pharm. Des.* **2007**, *20*, 2087−2100.
(13) Engel, C. K.; Pirard, B.; Schimanski, S.; Kirsch, R.; Habermann, J.; Klingler, O.; Schlotte, V.; Weithmann, K. U.; Wendt, K. U. Structural basis for the highly selective inhibition of MMP-13. *Chem. Biol.* **2005**, *2*, 181−189.
(14) Devel, L.; Czarny, B.; Beau, F.; Georgiadis, D.; Stura, E.; Dive, V. Third generation of matrix metalloprotease inhibitors: Gain in selectivity by targeting the depth of the S1′ cavity. *Biochimie* **2010**, *11*, 1501−1508.
(15) (a) Wu, J.; Rush, T. S. 3rd; Hotchandani, R.; Du, X.; Geck, M.; Collins, E.; Xu, Z. B.; Skotnicki, J.; Levin, J. I.; Lovering, F. E. Identification of potent and selective MMP-13 inhibitors. *Bioorg. Med. Chem. Lett.* **2005**, *18*, 4105−4109. (b) Monovich, L. G.; Tommasi, R. A.; Fujimoto, R. A.; Blancuzzi, V.; Clark, K.; Cornell, W. D.; Doti, R.; Doughty, J.; Fang, J.; Farley, D.; Fitt, J.; Ganu, V.; Goldberg, R.; Goldstein, R.; Lavoie, S.; Kulathila, R.; Macchia, W.; Parker, D. T.; Melton, R.; O'Byrne, E.; Pastor, G.; Pellas, T.; Quadros, E.; Reel, N.; Roland, D. M.; Sakane, Y.; Singh, H.; Skiles, J.; Somers, J.; Toscano, K.; Wigg, A.; Zhou, S.; Zhu, L.; Shieh, W. C.; Xue, S.; McQuire, L. W. Discovery of potent, selective, and orally active carboxylic acid based inhibitors of matrix metalloproteinase-13. *J. Med. Chem.* **2009**, *11*, 3523−3538. (c) Levin, J. I.; Chen, J. M.; Du, M. T.; Nelson, F. C.; Wehr, T.; DiJoseph, J. F.; Killar, L. M.; Skala, S.; Sung, A.; Sharr, M. A.; Roth, C. E.; Jin, G.; Cowling, R.; Di, L.; Sherman, M.; Xu, Z. B.; March, C. J.; Mohler, K. M.; Black, R. A.; Skotnicki, J. S. The discovery of anthranilic acid-based MMP inhibitors. *Bioorg. Med. Chem. Lett.* **2001**, *22*, 2975−2978. (d) Skiles, J. W.; Gonnella, N. C.; Jeng, A. Y. The design, structure, and clinical update of small molecular weight matrix metalloproteinase inhibitors. *Curr. Med. Chem.* **2004**, *11*, 2911−2977. (e) Rao, B. G. Recent developments in the design of specific Matrix Metalloproteinase inhibitors aided by structural and computational studies. *Curr. Pharm. Des.* **2005**, *11*, 295−322. (f) Wasserman, Z. R. Making a new turn in matrix metalloprotease inhibition. *Chem. Biol.* **2005**, *2*, 143−144.
(16) (a) Engel, C. K.; Pirard, B.; Schimanski, S.; Kirsch, R.; Habermann, J.; Klingler, O.; Schlotte, V.; Weithmann, K. U.; Wendt, K. U. Structural Basis for the Highly Selective Inhibition of MMP-13. *Chem. Biol.* **2005**, *12*, 181−189. (b) Klingler, O.; Kirsch, R.; Habermann, J.; Weithmann, K.-U.; Engel, C.; Pirard, B. Preparation of novel pyrimidine-4,6-dicarboxamides for the selective inhibition of collagenases. PCT Int. Appl. WO 2004041788, 2004. The crystal structure of the selective dicarboxamide pyrimidine MMP-13 inhibitor in complex with MMP-13 revealed a distinctive hydrogen-bonding network in the catalytic site. A structure-based virtual screening query was devised requiring hydrogen bonding to T245, T247, A238, and either to water 7 found in the cocrystal structure (PDB ID: 1XUD) or directly to M253. In addition, reaching either the S1′ or the S1′* pocket was required. Our internal compound collection was virtually screening against MMP-13 using Glide docking with constraints as described above yielding a hit set of approximately 15000 compounds. After clustering, visual inspection, and discarding structurally obvious analogues of known MMP-13 inhibitors, we chose 100 compounds to be tested for MMP-13 inhibition in a molecular assay.
(17) Salemme, F. R.; Spurlino, J.; Bone, R. Serendipity meets precision: the integration of structure-based drug design and combinatorial chemistry for efficient drug discovery. *Structure* **1997**, *3*, 319−324.
(18) (a) Heim-Riether, A.; Taylor, S. J.; Liang, S.; Gao, D. A.; Xiong, Z.; August, M. E.; Collins, B. K.; Farmer, B. T. 2nd; Haverty, K.; Hill-Drzewi, M.; Junker, H. D.; Margarit, M. S.; Moss, N.; Neumann, T.; Proudfoot, J. R.; Keenan, L. S.; Sekul, R.; Zhang, Q.; Li, J.; Farrow, N. A. Improving potency and selectivity of a new class of non-Zn-chelating MMP-13 inhibitors. *Bioorg. Med. Chem. Lett.* **2009**, *18*, 5321−5324. (b) Gao, D. A.; Xiong, Z.; Heim-Riether, A.; Amodeo, L.; August, E. M.; Cao, X.; Ciccarelli, L.; Collins, B. K.; Harrington, K.; Haverty, K.; Hill-Drzewi, M; Li, X.; Liang, S.; Margarit, S. M.; Moss, N.; Nagaraja, N.; Proudfoot, J.; Roman, R.; Schlyer, S.; Keenan, L. S.; Taylor, S.; Wellenzohn, B.; Wiedenmayer, D.; Li, J.; Farrow, N. A. SAR studies of non-zinc-chelating MMP-13 inhibitors: Improving selectivity and metabolic stability. *Bioorg. Med. Chem. Lett.* **2010**, *17*, 5039−5043.
(19) Boger, D. L. Preparation of CBI analogues of the duocarmycins and CC-1065 as antitumor agents with DNA alkylating activity. PCT Int. Appl. WO2004101767, 2004; 144.
(20) Yasuma, T.; Ujikawa, O.; Iwata, H. Preparation of indoles and related compounds as glucokinase activators. PCT Int. Appl. WO2006112549, 2006; 379 pp.